HHS Public Access

Author manuscript

Glia. Author manuscript; available in PMC 2020 June 01.

Published in final edited form as:

Glia. 2019 June ; 67(6): 1076–1093. doi:10.1002/glia.23589.

$G_{i/o}$ PROTEIN-COUPLED RECEPTORS INHIBIT NEURONS BUT ACTIVATE ASTROCYTES AND STIMULATE GLIOTRANSMISSION

Caitlin A. Durkee[1,2], **Ana Covelo**[1,2], **Justin Lines**[1], **Paulo Kofuji**[1], **Juan Aguilar**[3], and **Alfonso Araque Dr.**[1,*]

[1]Department of Neuroscience, University of Minnesota, Minneapolis, MN 55455, USA

[2]Equal contribution

[3]Hospital Nacional de Parapléjicos, SESCAM, Toledo, Spain

Abstract

G protein-coupled receptors (GPCRs) play key roles in intercellular signaling in the brain. Their effects on cellular function have been largely studied in neurons, but their functional consequences on astrocytes are less known. Using both endogenous and chemogenetic approaches with DREADDs, we have investigated the effects of G_q and $G_{i/o}$ GPCR activation on astroglial Ca^{2+}-based activity, gliotransmitter release, and the functional consequences on neuronal electrical activity. We found that while G_qGPCR activation led to cellular activation in both neurons and astrocytes, $G_{i/o}$GPCR activation led to cellular inhibition in neurons and cellular activation in astrocytes. Astroglial activation by either G_q or $G_{i/o}$ protein-mediated signaling stimulated gliotransmitter release, which increased neuronal excitability. Additionally, activation of G_q and $G_{i/o}$ DREADDs *in vivo* increased astrocyte Ca^{2+} activity and modified neuronal network electrical activity. Present results reveal additional complexity of the signaling consequences of excitatory and inhibitory neurotransmitters in astroglia-neuron network operation and brain function.

Keywords

astrocytes; G protein-coupled receptors; DREADDs; gliotransmission; astrocyte Ca^{2+}

INTRODUCTION

Intercellular chemical communication in the brain is based on neurotransmitters released by neurons and neurotransmitter receptors in the target cells, which upon activation can enhance or inhibit cellular activity. Two major classes of neurotransmitter receptors are responsible for transducing the intercellular chemical signaling – ligand-gated channels with ionotropic function that directly change membrane ionic permeability, and G protein-

AUTHOR CONTRIBUTIONS

A.A., A.C., and C.A.D. contributed to project conception, project design, and manuscript writing. A.C., C.A.D. and J.L. performed the experiments and analyzed the results. J.A. helped analyze the *in vivo* results. P.K. performed immunohistochemistry.

*Lead contact: Dept. Neuroscience, University of Minnesota, 4-110 Wallin Medical Biosciences Building, 2101 6th Street SE Minneapolis, MN 55455, Phone: (612) 624 0901, araque@umn.edu

DECLARATION OF INTERESTS

The authors declare no competing interests.

coupled receptors (GPCRs) with metabotropic function that activate intracellular signaling pathways. G proteins can be classified into four major families (i.e. G_s, G_q, $G_{i/o}$, $G_{12/13}$) according to the downstream signaling triggered by the activation of their α subunit. Briefly, some of the main signaling pathways are as follows: G_q activates phospholipase C (PLC), $G_{i/o}$ decreases cyclic AMP levels through inhibition of adenylyl cyclase, G_s stimulates adenylyl cyclase, and $G_{12/13}$ regulates small GTPases (Huang & Thathiah, 2015; Stewart & Fisher, 2015). Although there are a multitude of effects downstream of G protein activation, the classical view of G_q and $G_{i/o}$ protein signaling in neurons is excitation and inhibition, respectively (Huang & Thathiah, 2015). Whether these functional consequences of different G protein-mediated signaling occurs in other brain cells, like astrocytes, remains largely unknown.

Astrocytes are emerging as important cells in brain function by exchanging signaling with neurons through their participation in the tripartite synapse (Araque, Parpura, Sanzgiri, & Haydon, 1999). Rather than exhibiting electrical excitability like neurons, astrocytes display a form of excitability based on changes in intracellular Ca^{2+} concentration (Araque, Carmignoto, & Haydon, 2001; Araque et al., 2014; Di Castro et al., 2011; Haydon & Carmignoto, 2006; Mariotti et al., 2018; Navarrete & Araque, 2010; Panatier et al., 2011; Perea & Araque, 2005; Perea et al., 2016; Perea, Navarrete, & Araque, 2009; Verkhratsky & Kettenmann, 1996; Volterra, Liaudet, & Savtchouk, 2014; Volterra & Meldolesi, 2005). Upon activation, astrocytes can release their own signaling molecules, termed gliotransmitters, that regulate neuronal excitability, synaptic transmission, and plasticity (Araque et al., 2014; Bezzi et al., 2004; Halassa & Haydon, 2010; Rusakov, 2015; Volterra & Meldolesi, 2005) see however (Fiacco & McCarthy, 2018). A major route of inducing Ca^{2+} elevations is through activation of G_q GPCRs that results in the release of Ca^{2+} from internal stores through activation of PLC and IP_3 receptors (IP_3R) (Di Castro et al., 2011; Panatier et al., 2011; Pasti, Volterra, Pozzan, & Carmignoto, 1997; Perea & Araque, 2005; Porter & McCarthy, 1996). The effects of $G_{i/o}$ GPCR activation in astrocytes are less known. Reports indicate that neurotransmitter receptors typically coupled to $G_{i/o}$ GPCRs, such as CB1 and $GABA_B$ receptors, can increase Ca^{2+} levels and stimulate gliotransmission (Covelo & Araque, 2018; Kang, Jiang, Goldman, & Nedergaard, 1998; Mariotti, Losi, Sessolo, Marcon, & Carmignoto, 2016; Meier, Kafitz, & Rose, 2008; Navarrete & Araque, 2008; Perea et al., 2016). While CB1 receptors have been shown to promiscuously couple to G_q proteins (Lauckner, Hille, & Mackie, 2005; Navarrete & Araque, 2008), whether $G_{i/o}$ protein activation inhibits cellular activity in astrocytes, like in neurons, remains unclear.

Here, we have investigated the functional consequences of selective activation of G_q and $G_{i/o}$ GPCRs on astrocytic and neuronal activity using endogenous and chemogenetic (i.e. Designer Receptors Exclusively Activated by Designer Drugs, DREADDs) approaches. Combining electrophysiological and Ca^{2+} imaging techniques in hippocampal mouse brain slices, we found that G_q GPCR activation in both neurons and astrocytes led to cellular activation. Hereafter, cellular activation is defined as calcium increases in both neurons and astrocytes and depolarization in neurons. In contrast, $G_{i/o}$ GPCR activation inhibited neurons, but led to astrocyte activation. Furthermore, G_q or $G_{i/o}$ GPCR activation in astrocytes stimulated the release of glutamate, which enhanced neuronal excitability. Activation of both G_q and $G_{i/o}$ DREADDs in astrocytes of the primary somatosensory cortex

in vivo similarly led to the enhancement of both astrocyte Ca^{2+} elevations and cortical delta rhythms. These results indicate that while activation of different GPCR pathways in neurons led to either excitation or inhibition, in astrocytes they led only to activation, suggesting that inhibitory signaling is a particular property of neurons and not astrocytes.

METHODS

Experimental model and subject details

Hippocampal coronal slices were obtained from both male and female 6–12 weeks old C57BL/6, GCaMP3 (GLAST-CreE RT2 x R26-lsl-GCaMP3; (Paukert et al., 2014)), GCaMP6f (Tg(Slc1a3-cre/ERT)1Nat/J (JAX:012586) x Ai95(RCL-GCaMP6f)-D (JAX: 028865); (Agarwal et al., 2017) and $IP_3R2^{-/-}$ (Li, Zima, Sheikh, Blatter, & Chen, 2005) mice. GCaMP3 mice received 8 daily doses (57mg/kg) of tamoxifen injections two weeks prior to experimentation. Mice were housed in a 14/10 light/dark cycle with ad libitum food and water. All experiments were in compliance with the Animal Care and Use Committee at the University of Minnesota.

Stereotaxic surgery

4–6-week-old mice were anesthetized with ketamine/xylazine (10 ml/kg) and underwent stereotaxic surgery of AAV5-CaMKIIα-hM3Dq or AAV5-CaMKIIα-hM4Di to assess G_q and $G_{i/o}$ signaling in neurons, respectively, or AAV8-GFAP-hM3Dq or AAV8-GFAP-hM4Di to assess G_q and $G_{i/o}$ signaling in astrocytes, respectively. Stereotaxic coordinates used for all hippocampal injections were (relative to Bregma in mm) −2.65 A-P, ±2.25 M-L and −1.75 D-V. Stereotaxic coordinates used for all *in vivo* cortical injections were (relative to Bregma in mm): −−2.00 A-P, ±2.00 M-L and −1.00, −0.80, and −0.60 D-V. For *in vivo* control experiments, mice underwent stereotaxic surgery of AAV8-GFAP-mCherry. Experiments were performed 2–6 weeks after surgery. All DREADDs viruses were purchased from the UNC Vector Core, while the plasmid to generate the AAV8-GFAP-mCherry was purchased from Addgene (Plasmid #58909) and was generated by the University of Minnesota Viral Vector and Cloning Core.

Hippocampal slice preparation

The brain was removed quickly after decapitation and placed in ice-cold artificial cerebrospinal fluid (ACSF). Coronal hippocampal slices (350um thick) were made with a vibratome and incubated (>1 h) in a holding chamber at room temperature (21–24 degrees C) in ACSF containing (in mM): NaCl 124, KCl 2.69, KH2PO4 1.25, $MgSO_4$ 2, $NaHCO_3$ 26, $CaCl_2$ 2, ascorbic acid 0.4, and glucose 10, and continuously bubbled with carbogen (95% O2 and 5% CO_2) (pH 7.3). Slices were transferred to an immersion recording chamber and superfused at 2mL/min with gassed magnesium-free ACSF containing (in mM): NaCl 124, KCl 2.69, KH_2PO_4 1.25, $NaHCO_3$ 26, $CaCl_2$ 4, glucose 10, and glycine 4. Tetrodotoxin (TTX, 1μM) was included in the perfusion system for all slice experiments to block action potential-mediated neurotransmission, except for experiments in Figure 7. To isolate GABAB receptor-mediated events in the GABA application experiments, picrotoxin (GABAA receptor antagonist, 50 μM) was added to the perfusion system. In experiments to block G_q-PLC signaling, the PLC inhibitor U73122 (4 μM) was included in the perfusion

system. In experiments to block $G_{i/o}$ signaling, slices were incubated in ACSF containing the $G_{i/o}$ inhibitor pertussis toxin (PTX; 7.5 μg/ml) for 3–4 hours prior to experiments. In experiments to block muscarinic ACh receptors, atropine (50 μM) was included in the perfusion system. In experiments to block GABAB receptors, CGP54626 (1 mM) was included in the perfusion system. Cells were visualized under 40x water immersion objective using differential interface contrast (DIC) in an Olympus microscope.

Slice electrophysiology

Whole-cell electrophysiological recordings were performed in pyramidal neurons of the CA1 region of the hippocampus. Patch pipettes were pulled from thick-walled borosilicate glass (1.5 mm outer diameter) on a Sutter Instruments P-1000 puller. Pipettes (3–8 MΩ) were filled with the internal solution that contained (in mM): K-Gluconate 135, KCl 10, HEPES 10, MgCl2 1, ATP-Na2 2 (pH = 7.3 adjusted with KOH; osmolality 280–290 mOsm/L). Recordings were obtained and filtered (1KHz) by PC-ONE amplifiers (Dagan Instruments, Minneapolis, MN). Signals were fed to a Pentium-based PC through a DigiData 1440A interface board. The pCLAMP 10.2 (Axon Instruments) software was used for stimulus generation, data display, acquisition and storage. For neuronal DREADDs experiments, only mCherry-positive CA1 neurons were patched, and mCherry-negative neurons were recorded for sham conditions. For neuronal slow inward current (SIC) and action potential firing responses after astrocytic DREADDs activation, only mCherry-positive slices were used, and mCherry-negative slices were used for sham conditions. ACh- and CNO-evoked neuronal currents and SICs were recorded in voltage-clamp at a holding potential of −70mV and GABA-mediated currents were recorded at a holding potential of −40mV. To mimic excitatory inputs and observe changes in action potential firing over time (Figure 7), a continuous train of depolarizing current pulses (20ms, ~200 pA, delivered every 50ms) was applied. SICs were defined as currents with a $\tau_{on} > 5$ and lasting > 40ms. Experiments were performed at room temperature (21–24 °C).

Agonist application

For all slice agonist application experiments, pipettes (3–8 MΩ) were filled with ACSF plus 1 mM ACh or 1 mM GABA or 1 mM CNO, or 2mM (*S*)-3,5-Dihydroxyphenylglycine (DHPG). Pipettes were positioned over the pyramidal layer to assess neuronal responses to the agonist (Figures 1, 3), or over the stratum radiatum to assess astrocytic Ca^{2+} response to agonist application, SICs, and firing modulation (Figures 2, 4-7). To illustrate the time course of the agonist effects on SIC frequency in Figure 6, the number of SICs were grouped in 10s bins. To compare the agonist effects, the mean SIC frequency recorded 1 minute before and after agonist application was calculated. Agonists were delivered using a Dagan PMI-100 Pressure Micro-injector (15 PSI, 2–5s for all experiments except for the following: 30s for chemogenetic SIC experiments and firing modulation experiments).

Ca^{2+} imaging

Ca^{2+} levels in astrocytes were monitored by two-photon microscopy (Leica DM6000 CFS upright multiphoton microscope with TCS SP5 MP laser) using the genetically encoded Ca^{2+} indicator mice GCaMP3 and GCaMP6 expressed in GLAST-positive cells. Some (n=199/512) soma Ca^{2+} responses were monitored by an Olympus BX51W1 epifluorescent

microscope using Fluo-4-AM (5 μM in 0.01% of pluronic, 45min incubation at room temperature). Astrocytic Ca^{2+} levels were recorded from the astrocyte cell body and processes, and Ca^{2+} variations were estimated as changes in the fluorescence signal over the baseline ($\Delta F/F_0$). A Ca^{2+} signal was considered a Ca^{2+} event when F/F_0 >3 standard deviations greater than baseline fluorescence. Our measurement of Ca^{2+} event probability was calculated as the number of Ca^{2+} elevations grouped in 5s bins recorded from the astrocytes in the field of view (3–6 astrocytes per analyzed region), and mean values were obtained by averaging each different experiment. References to "n" in the text correspond to the number of experiments performed for each condition. Ca^{2+} analysis was performed only on astrocyte soma and processes within the field of view that showed fluctuations in Ca^{2+} levels throughout the recording. A domain was only selected along an active process length if its activity pattern differed from neighboring regions, so as to avoid oversampling of an active process. The number of process domains per experiment was 16.6 ± 0.48. Ca^{2+} levels in neurons were monitored using bulk loading of Oregon Green BAPTA-1 (5 μM in 0.01% of pluronic, 1hr incubation at room temperature) or adding Fluo4 (50 μM) to the recording pipette. A change in fluorescence ($\Delta F/F_0$ > 3 standard deviations from baseline fluorescence) occurring within 5s of agonist application was defined as a neuronal Ca^{2+} response.

In vivo experiments and analysis

Two- to six-month-old mice were anesthetized using 1.8 mg/kg urethane injected intraperitoneally, faux tears were applied, and body temperature was maintained at 37°C. Once anesthetized, animals were placed in a stereotaxic frame and a midline incision was made along the scalp. A 3mm diameter craniotomy was performed centered over the primary somatosensory cortex (relative to Bregma in mm: −2.00 A-P, −2.00 M-L). A 0.25mm tungsten wire was placed over the exposed cortex to measure electrocorticography (ECoG), and agar was applied before a glass coverslip was cemented atop the craniotomy. A screw soldered to wire was inserted over the cerebellum to act as the reference and another screw was placed over the ipsilateral frontal plate. A 3D printed frame was mounted to the exposed skull with dental acrylic and fastened to a holder. The holder and animal were then placed underneath a Leica SP5 two-photon microscope for imaging. ECoG was recorded by connecting the lead to the exposed wire over the cortical surface, and reference and ground were attached to the wire soldered to the screw placed over the cerebellum. Prior to data acquisition, a needle was fed into the intraperitoneal cavity connected to a syringe with CNO. ECoG was sent to an AM Systems 3000 AC/DC differential amplifier sampled at 10kHz, filtered at 1Hz-3kHz and digitized using an Axon Digidata 1550 Acquisition System connected to a Dell Optiplex 7010 PC. In this arrangement, ECoG was recorded simultaneously with astrocyte Ca^{2+} monitored in cortical layers 2/3 (i.e. 100–300 μm below the cortical surface). Ca^{2+} imaging was obtained at 1 frame per second through a 25X objective with an additional 1.7X digital zoom. Following 20 minutes of baseline, 2–3 mg/kg CNO was injected intraperitoneally. Following CNO injections, measurements were obtained for 90 minutes. In a subset of mice, ECoG was measured in the absence of Ca^{2+} imaging. Raw ECoG data was lowpass filtered at 300 Hz and analyzed using a custom MATLAB program where a short-time Fourier transform was done using a hamming window to measure spectral content every minute. Normalized ECoG power spectra were

created by using min-max normalization with respect to the baseline. *In vivo* Ca^{2+} data was analyzed using a custom MATLAB program to detect Ca^{2+} events via change in fluorescence, or the derivative of the fluorescence, when the derivative of fluorescence was > 2 standard deviations of the baseline speed over the average baseline speed. After an event was detected, the program detected the end of the event when the trace decayed back to the onset amplitude; from this the duration of the event was quantified, and the amplitude was calculated by taking the maximum value between onset and decay and subtracting it from the amplitude of the onset.

Immunohistochemistry

Anesthetized mice were perfused through the left cardiac ventricle with 4% paraformaldehyde in 0.1M PBS. The brains were removed, postfixed with paraformaldehyde and cut into 50 μm slices using a Leica VT 1000S vibratome. Brain sections were blocked with phosphate-buffered saline (PBS) containing 10% normal goat serum (NGS) or normal donkey serum (NDS) and 0.2% Triton X-100 and incubated overnight with the primary antibody diluted in blocking solution. Appropriate fluorochrome-labeled secondary antibodies (Life Technologies, Waltham, MA) were used for detection. An antibody against glial fibrillary acidic protein (GFAP, 1:1000; Sigma-Aldrich) was used as a marker for astrocytes. An antibody against neuron-specific nuclear protein (NeuN, 1:500; Millipore) was used as a marker for neurons. Fluorescent stained sections were mounted with Vectashield mounting medium (Vector Laboratories). The stained sections were visualized with a Nikon NiE C2 or an Olympus FluoView FV1000 upright confocal microscope and analyzed for colocalization of DREADDs with either neurons or astrocytes using ImageJ software (NIH, Bethesda, MD).

Quantification and statistical analyses

Data are expressed as mean ± standard error of the mean (SEM). Data normal distribution was assessed using a Shapiro-Wilk Normality test. Ca^{2+} event probability, Ca^{2+} fluorescence, SIC frequency, and *in vivo* Ca^{2+} events were analyzed using a two-tailed paired Student's t-test ($\alpha = 0.05$) comparing baseline to post-stimulus. *In vivo* delta power was analyzed using a Wilcoxon signed-rank test ($\alpha = 0.05$) comparing baseline to post-stimulus. A one-way ANOVA was used with Holm-Sidak posthoc test to compare treatment groups against the control group for neuronal electrophysiology response data. When the Shapiro-Wilk Normality test failed, a Kruskal-Wallis ANOVA with a Dunn's posthoc was used. Statistical differences were established with $P < 0.05$ (*), $P < 0.01$ (**), and $P < 0.001$ (***).

RESULTS

G_q GPCR activation in neurons

We first investigated the effects on neurons of endogenous G_q GPCR activation by acetylcholine (ACh), which activates muscarinic ACh receptors (mAChRs). Type 1, 3 and 5 mAChRs, known to be coupled to G_q proteins, are highly expressed in hippocampal neurons (Berkeley et al., 2001; Park & Spruston, 2012; Scheiderer et al., 2008). We performed whole-cell electrophysiological recordings from hippocampal CA1 pyramidal neurons,

monitored neuronal Ca^{2+} levels, and locally applied ACh (Figure 1A). CA1 neurons responded to ACh with an inward current in voltage clamp conditions, a transient depolarization in current clamp, and Ca^{2+} elevations (n = 9; Figures 1B–1E). These responses were abolished by the mAChR antagonist atropine (50 μM; n = 5; Figures 1C and 1E). Furthermore, ACh-evoked responses were prevented by the PLC inhibitor U73122 (4 μM; n = 7), but present after incubation with the $G_{i/o}$ inhibitor pertussis toxin (7.5 μg/ml; PTX; n = 6; Figures 1C and 1E), which is consistent with the canonical G_q signaling pathway (Huang & Thathiah, 2015; Stewart & Fisher, 2015). These results indicate that ACh-induced activation of G_q GPCR signaling evokes neuronal responses (i.e. inward currents and Ca^{2+} increases) associated with neuronal excitation.

To confirm the effects of G_q signaling in neurons, we selectively expressed G_qDREADDs in hippocampal CA1 pyramidal neurons using the viral vector AAV5-CaMKIIα-hM3Dq-mCherry, which contains the G_qDREADD and the fluorescent reporter mCherry under the CaMKIIα promoter, which is highly expressed in CA1 pyramidal neurons (Erondu & Kennedy, 1985; Schulman & Lou, 1989). The selective expression of G_qDREADDs in CA1 pyramidal neurons was confirmed by immunohistochemistry (Figure 1F) and the electrophysiological properties of the recorded neurons expressing mCherry (Gasparini & Magee, 2006; Magee & Carruth, 1999). Local application of the DREADD agonist Clozapine-N-oxide (CNO) evoked transient depolarizations, inward currents, and Ca^{2+} increases in G_qDREADD-expressing neurons (n = 8; Figures 1G–1K), but not in neurons lacking G_qDREADDs (n = 6; Figures 1I and 1K). CNO-evoked responses were diminished by U73122 (n = 5), but not by PTX (n = 6; Figures 1I and 1K). These results indicate that G_q activation by endogenous or chemogenetic means induces neuronal responses associated with cellular excitation.

G_q GPCR activation in astrocytes

Hippocampal astrocytes respond with Ca^{2+} elevations to ACh through activation of mAChRs (Araque, Martin, Perea, Arellano, & Buno, 2002; Shelton & McCarthy, 2000), but the signaling pathway activated remains undefined. Thus, we locally applied ACh and monitored Ca^{2+} levels in the soma and processes of astrocytes located in the CA1 *stratum radiatum* using transgenic mice that expressed the genetically-encoded Ca^{2+} indicators GCaMP3 or GCaMP6 under the astroglial GLAST promoter (Figure 2A). ACh transiently elevated Ca^{2+} in both astrocyte somas and processes (Figures 2B-E) (Araque et al., 2002; Navarrete et al., 2012; Perea & Araque, 2005; Shelton & McCarthy, 2000; Takata et al., 2011), as quantitatively shown by the increase of the Ca^{2+} event probability (36 astrocyte somas, n = 6; 122 process domains, n = 5; Figures 2D–2E). ACh-induced Ca^{2+} increases were blocked by the mAChR antagonist atropine (18 astrocyte somas, n = 6; 78 process domains, n = 6; Figures 2D and 2E) and by the PLC inhibitor U73122 (27 astrocyte somas, n = 7; 106 process domains, n = 7; Figures 2D and 2E), but were present in slices incubated with the $G_{i/o}$ inhibitor PTX (54 astrocyte somas, n = 9; 83 process domains, n = 7; Figures 2D and 2E). These results indicate that mAChRs in astrocytes activate G_q proteins that increase intracellular Ca^{2+} levels through stimulation of PLC.

To selectively stimulate G_q-linked GPCRs in astrocytes, we targeted *stratum radiatum* hippocampal astrocytes with the viral vector AAV8-GFAP-hM3Dq-mCherry, which contains the G_qDREADD and the fluorescent reporter mCherry under the control of the astroglial GFAP promoter (Figure 2F). CNO application mimicked the ACh effects, elevating Ca^{2+} in both somas and processes of G_qDREADD-expressing astrocytes (35 astrocyte somas, n = 6; 153 process domains, n = 6; Figures 2G–2K), but not in astrocytes lacking G_qDREADD expression (18 astrocyte somas, n = 6; 100 process domains, n = 6; Figures 2J and 2K). CNO-evoked responses in both somas and processes were blocked by U73122 (20 astrocyte somas, n = 5; 83 process domains, n = 6), but were still present in slices incubated with PTX (18 astrocyte somas, n = 5; 53 process domains, n = 5; Figures 2J and 2K), indicating that G_q GPCR signaling pathways increase Ca^{2+} in astrocytes by activation of PLC. To further test this idea and to determine the source of the Ca^{2+} elevation and the intracellular signaling downstream of G_qDREADD activation, we performed the experiment in $IP_3R2^{-/-}$ mice (Li et al., 2005), which lack type 2 IP_3 receptors, the main receptor subtype responsible for astrocytic Ca^{2+} mobilization from internal stores (Di Castro et al., 2011; Gomez-Gonzalo et al., 2015; Martin-Fernandez et al., 2017; Martin, Bajo-Graneras, Moratalla, Perea, & Araque, 2015; Navarrete et al., 2012; Petravicz, Fiacco, & McCarthy, 2008). CNO application in G_qDREADD-expressing slices from $IP_3R2^{-/-}$ mice showed no significant increase in Ca^{2+} event probability (14 astrocyte somas, n = 5; 46 process domains, n = 5; Figures 2J and 2K), indicating that G_q-GPCR activation induces astrocyte Ca^{2+} mobilization from internal stores. Taken together, these results indicate that stimulating G_q GPCR signaling evokes astrocyte responses (i.e. Ca^{2+} increases) associated with astrocyte activation.

$G_{i/o}$ GPCR activation in neurons

To investigate $G_{i/o}$ signaling cascade effects on neurons, we used GABA to activate endogenous $GABA_B$ receptors, which are known to be coupled to $G_{i/o}$ proteins (Logothetis, Kurachi, Galper, Neer, & Clapham, 1987; North, 1989; Wickman et al., 1994). $GABA_B$-mediated responses were isolated by blocking $GABA_A$ receptors with picrotoxin (50 μM). In CA1 pyramidal neurons, GABA application evoked a hyperpolarization in current-clamp conditions, and an outward current in voltage-clamp conditions (n = 8; Figures 3A and 3B), with no changes in Ca^{2+} levels (n = 6; see Figure 3C). The outward currents were blocked by the $GABA_B$ receptor antagonist CGP54626 (1 mM; n = 5), as well as by the $G_{i/o}$ inhibitor PTX (n = 5), but were unchanged by the PLC inhibitor U73122 (n = 5; Figure 3B). These data indicate that $G_{i/o}$ intracellular signaling cascades evoke effects (i.e. outward currents and absence of Ca^{2+} increases) consistent with neuronal inhibition.

We further investigated the effects of neuronal $G_{i/o}$-linked GPCRs using the $G_{i/o}$DREADD (Armbruster, Li, Pausch, Herlitze, & Roth, 2007), which was specifically expressed in CA1 pyramidal neurons with the viral vector AAV5-CaMKIIα-hM4Di-mCherry (Figure 3D and 3E). CNO application hyperpolarized and evoked outward currents in $G_{i/o}$DREADD-expressing neurons (n = 7), but not in neurons lacking $G_{i/o}$DREADD expression (n = 5; Figure 3F). These effects were absent in PTX-incubated slices (n = 5), but were similar to control in the presence of U73122 (n = 5; Figure 3F). Like GABA, CNO did not modify

Ca^{2+} levels (n = 6; see Figure 3G). These data indicate that $G_{i/o}$ signaling evoked by GABA or DREADDs has inhibitory actions on neurons.

$G_{i/o}$ GPCR activation in astrocytes

We then tested the effects of $G_{i/o}$GPCR stimulation on astrocyte Ca^{2+} activity. Local application of GABA increased the Ca^{2+} event probability in both somas and processes (49 astrocyte somas, n = 10; 147 process domains, n = 7; Figures 4A–4E). These effects were not observed in PTX-treated slices (57 astrocyte somas, n = 9; 69 processes domains, n = 5; Figures 4D and 4E) or in the presence of the $GABA_B$ receptor antagonist CGP54626 (26 astrocyte somas, n = 5; 61 process domains, n = 6; Figures 4D and 4E), but were still present in U73122 conditions (38 astrocyte somas, n = 8; 161 process domains, n = 5; Figures 4D and 4E), indicating that, unlike in neurons, stimulation of $G_{i/o}$GPCR signaling in astrocytes leads to cellular activation.

To further test this hypothesis, $G_{i/o}$DREADDs were specifically expressed in astrocytes using the viral vector AAV8-GFAP-hM4Di-mCherry (Figure 4F). CNO application transiently increased the Ca^{2+} event probability in somas and processes of $G_{i/o}$DREADD-expressing astrocytes (21 astrocyte somas, n = 5; 163 process domains, n = 8), but not in non-expressing astrocytes (19 astrocyte somas, n = 5; 71 process domains, n = 5; Figures 4G–4K). These Ca^{2+} responses were present in U73122 (20 astrocyte somas, n = 5; 160 process domains, n = 6), but were absent in PTX-treated slices (20 astrocyte somas, n = 6; 144 process domains, n = 6), and in slices from $IP_3R2^{-/-}$ mice (22 astrocyte somas, n = 5; 48 process domains, n = 5; Figures 4J and 4K). Taken together, these results indicate that $G_{i/o}$ signaling evoked by endogenous and chemogenetic approaches resulted in astrocyte activation manifested as Ca^{2+} increases.

Simultaneous activation of G_q and $G_{i/o}$ GPCR signaling in astrocytes

We further tested the hypothesis that G_q and $G_{i/o}$ GPCR signaling in astrocytes operates through distinct intracellular pathways. We hypothesized that two agonists acting on similar GPCR signaling pathways would interact producing a non-linear response, whereas two agonists activating different GPCR signaling would evoke a linear response. We first tested two agonists that are known to activate G_q GPCR signaling, ACh and group I mGluR agonist (*S*)-3,5-Dihydroxyphenylglycine (DHPG). We either applied them separately or both simultaneously and monitored the Ca^{2+} responses. We found that the observed Ca^{2+} response elicited by the simultaneous ACh and DHPG application was lower than the response expected if there was no interaction; i.e., the linear summation of the peak Ca^{2+} elevation evoked by each agonist applied separately (n = 26; Figures 5A, 5B, and 5E) (Perea & Araque, 2005). This relative reduction of the response evoked by these agonists indicates an interaction of the signaling pathways activated and suggests that they operated through the same intracellular pathways. Next, we applied separately ACh, GABA, or both simultaneously to measure the relative contribution of G_q and $G_{i/o}$ GPCR signaling, respectively, to the astrocyte Ca^{2+} response. We found that the observed amplitude of the Ca^{2+} response to simultaneous ACh and GABA application was similar to that of the expected response; i.e., the linear summation of the responses evoked independently (n = 29; Figures 5C, 5D, and 5E). Moreover, the peak amplitude of the Ca^{2+} response could be

further increased by increasing the concentration of ACh (peak fluorescence evoked by 1 mM ACh: 39.4 ± 4.8%, peak fluorescence evoked by 10 mM ACh: 64.6 ± 8.3%, p = 0.040, n = 4 videos, 13 astrocytes), indicating that the receptors and signaling pathways were not saturated. The fact that the Ca^{2+} response linearly summated with simultaneous G_q and $G_{i/o}$ GPCR agonist application suggests that distinct intracellular pathways were activated, indicating that the actions of $G_{i/o}$ and G_q GPCRs do not occlude and that the detected Ca^{2+} signal is not saturated. Furthermore, these results indicate that two distinct intracellular signaling mechanisms are activated downstream of G_q and $G_{i/o}$ GPCR signaling in astrocytes.

Downstream effects of astrocytic G_q and $G_{i/o}$ GPCR activation on neurons

Next, we investigated whether activation of G_q and $G_{i/o}$ protein signaling in astrocytes can lead to gliotransmitter release and regulation of neuronal excitability. Astrocyte Ca^{2+} elevations have been shown to stimulate the release of glutamate, which evokes slow inward currents (SICs) mediated by activation of neuronal NMDA receptors (Araque, Parpura, Sanzgiri, & Haydon, 1998; Araque et al., 1999; Araque, Sanzgiri, Parpura, & Haydon, 1998; Fellin et al., 2004; Mariotti et al., 2016; Martin et al., 2015; Navarrete & Araque, 2008; Perea & Araque, 2005; Perea, Sur, & Araque, 2014). SICs can be distinguished from synaptic currents by their different time courses and their sensitivity to the NMDA receptor antagonist D-AP5 (50 μM; average SIC amplitude = 19.7 pA ± 1.6 pA; n = 182; Figures 6A–6C). We used SICs as a biological assay to detect astrocytic glutamate release. ACh application, which increased astrocyte Ca^{2+} via G_q protein activation (see Figure 2), transiently increased the frequency of SICs in CA1 pyramidal neurons (n = 11; Figures 6D and 6E). In correspondence with the ACh-evoked effects on Ca^{2+}, this effect was blocked by atropine (n = 5) and U73122 (n = 7), but was present in PTX-treated slices (n = 5; Figure 6E). Similarly, CNO application in slices with G_qDREADD-expressing astrocytes transiently increased SIC frequency (n = 5), an effect that remained in PTX-treated slices (n = 4; Figures 6F–6G). This effect was absent in the presence of U73122 (n = 5), in sham conditions with no expression of DREADDs (n = 4), and in slices from $IP_3R2^{-/-}$ mice (n = 8; Figures 6G). These data indicate that G_q-linked GPCR activation in astrocytes stimulates the release of glutamate that activates neuronal NMDA receptors.

We then quantified the effects of $G_{i/o}$ GPCR activation on SIC frequency. GABA transiently increased the frequency of SICs (n = 9; Figures 6H and5I). As in the case of GABA-evoked Ca^{2+} responses, SIC frequency increases were abolished by CGP54626 (n = 5) and PTX (n = 6), but were detected in slices treated with U73122 (n = 9; Figure 6I). Likewise, CNO application in slices with $G_{i/o}$DREADD-expressing astrocytes increased SIC frequency in control conditions (n = 7) and in the presence of U73122 (n = 4), but this effect was absent in PTX-incubated slices (n = 5), in sham conditions (n = 5), and in slices from $IP_3R2^{-/-}$ mice (n = 8; Figures 6J and 6K). Taken together, G_q and $G_{i/o}$ GPCR activation in astrocytes led to increases in Ca^{2+}, which were associated with an increase in the number of SICs in nearby neurons.

SICs are proposed to enhance neuronal excitability and regulate neuronal synchronization (Angulo, Kozlov, Charpak, & Audinat, 2004; Fellin et al., 2004). We directly tested this idea

by investigating the effects of G_q and $G_{i/o}$ GPCR stimulation in astrocytes on action potential firing in nearby neurons (Figure 7). We activated G_q- and $G_{i/o}$DREADD-expressing astrocytes while recording hippocampal CA1 pyramidal neurons in current-clamp conditions. In a first approach, the neuronal membrane potential was slightly depolarized from resting membrane potential by injecting a continuous current to facilitate firing of spontaneous action potentials (Figures 7A and 7B). In a second approach, a continuous train of depolarizing current pulses (20ms, ~200 pA, delivered every 50ms) was applied to observe any potential changes in action potential firing (Figures 7C and 7D). In both conditions, CNO application to either G_q- or $G_{i/o}$DREADD-expressing astrocytes enhanced the frequency of action potential firing (Figures 7A–7D, and 7G-7H), which agrees with the gliotransmitter-evoked enhancement of neuronal excitability (see Figure 6). Indeed, the astrocyte G_q- and $G_{i/o}$DREADD effects on action potential firing were accompanied by small, but conspicuous, transient depolarizations (insets in Figures 7C and 7D), which appear consistent with the SICs recorded in voltage-clamp (see Figures 6F and 6J), although experimental limitations cannot provide direct evidence that SICs (recorded in voltage-clamp) are responsible for these depolarizations (recorded in current-clamp). Nevertheless, activation of both G_q- and $G_{i/o}$DREADDs in the presence of the NMDA receptor antagonist D-AP5 failed to evoke the previously observed transient depolarizations and increase in action potential firing (Figures 7E–7H), supporting the idea that these phenomena were due to neuronal NMDAR activation by astrocytic glutamate. Taken together, these results indicate that activation of both G_q and $G_{i/o}$ proteins activated astrocytes in the form of a Ca^{2+} elevation. This cellular activation in astrocytes subsequently stimulated gliotransmitter release that led to the enhancement of neuronal excitability.

Effects of astrocytic G_q and $G_{i/o}$ GPCR signaling *in vivo*

Finally, we investigated whether similar phenomena occurred *in vivo*. We injected the viral vectors AAV8-GFAP-hM3Dq-mCherry or AAV8-GFAP-hM4Di-mCherry into the primary somatosensory cortex to selectively express in cortical astrocytes G_q or $G_{i/o}$ DREADDs, respectively (Figure 8A). Two weeks after injection, we monitored astrocyte Ca^{2+} activity and cortical local field potentials in anesthetized mice, in basal conditions and 1 hour after intraperitoneal injection of CNO (2–3 mg/kg). In mice (n = 6) with G_qDREADD-expressing astrocytes, CNO increased the frequency (from 1.30 ± 0.06 to 2.70 ± 0.28 events/min; n = 21 astrocytes), amplitude (to 218.9 ± 31.2 % from basal values between each astrocyte), and duration of the Ca^{2+} events (from 2.84 ± 0.17 to 6.00 ± 0.69 s) (Figures 8B-8G). Similarly, CNO injection to mice (n = 6) with $G_{i/o}$DREADD-expressing astrocytes also increased the frequency (from 1.21 ± 0.08 to 2.00 ± 0.23 events/min; n = 24 astrocytes), amplitude (to 229.5 ± 32.724 % from basal values of each astrocyte), and duration of Ca^{2+} events (from 4.20 ± 0.79 to 6.62 ± 0.80 s) (Figures 8B-8G). Introducing saline into mice (n = 3) with G_qDREADD-expressing astrocytes did not increase the frequency (from 1.35 ± 0.05 to 1.30 ± 0.05 events/min in 37 astrocytes), amplitude (to 98.1 ± 6.0 % from basal values between astrocytes), or duration of the Ca^{2+} events (from 2.81 ± 0.11 to 2.80 ± 0.12 s). Similarly, introducing saline in mice (n = 3) with $G_{i/o}$-DREADD-expressing astrocytes did not increase frequency (from 1.30 ± 0.04 to 1.34 ± 0.06 events/min; n = 53), amplitude (to 114.8 ± 10.3 % from basal values between astrocytes), or duration (from 2.80 ± 0.10 to 2.83 ± 0.13 s) of the Ca^{2+} events. Additionally, introducing CNO in mice (n = 3) expressing mCherry in

astrocytes did not increase the frequency (from 1.32 ± 0.04 to 1.44 ± 0.06 events/min; n = 77), amplitude (to 118.7 ± 9.3 % from baseline between astrocytes), or duration of the Ca^{2+} events (from 2.78 ± 0.09 to 3.10 ± 0.16 s).

Associated with the CNO-evoked astrocyte activation, CNO altered the electrical network activity manifested as an enhancement of the slow-wave delta activity (0–4 Hz) in mice with astrocytes expressing either G_q or $G_{i/o}$DREADDs (n = 6 mice for each case; Figures 8H-8K). These effects were not observed when mice with either G_q or $G_{i/o}$DREADDs-expressing astrocytes were injected with saline (n=3 mice for each case; Figures 8F, 8G, 8J, and 8K), or when CNO was delivered to mice infected with the control virus GFAP-mCherry that lacks DREADDs (n=3 mice; Figures 8F, 8G, 8J, and 8K). These results indicate that *in vivo* activation of either G_q or $G_{i/o}$ GPCR signaling in astrocytes similarly led to the activation of astrocytes, and that these effects were associated with alterations of the neural delta network activity.

DISCUSSION

The present results show that G_q GPCR activation in neurons and astrocytes activated both cell types. In contrast, while neuronal $G_{i/o}$ GPCR activation inhibited cellular activity, $G_{i/o}$ GPCR stimulation in astrocytes enhanced their Ca^{2+}-based cellular activity. We found that activation of endogenous G_q or $G_{i/o}$ GPCRs or DREADDs in astrocytes induced Ca^{2+} increases in astrocyte somas and processes and stimulated the release of the gliotransmitter glutamate, which led to an increase in SIC frequency and action potential firing in hippocampal neurons, and impacted neuronal network activity *in vivo*. Hence, astrocyte G protein-mediated signaling, whether G_q or $G_{i/o}$, activated astrocytes by way of an evoked Ca^{2+} response. Therefore, neurotransmitters acting on $G_{i/o}$ GPCRs proteins directly inhibit neurons but activate astrocytes, which then can feed-forward excite neurons. Consistent with this idea, we have found that astrocyte specific G_q or $G_{i/o}$ GPCR activation enhanced astrocyte Ca^{2+} events and delta activity *in vivo*. These results add further complexity to the signaling mechanisms and effects of GPCR-mediated signaling in the brain, revealing important and unexpected functional consequences on the actions of inhibitory neurotransmitters in astroglial-neuronal networks.

Our results show that neuronal G_q GPCR activation either with ACh or G_qDREADDs increase neuronal excitability, both inducing inward currents, membrane depolarizations, and Ca^{2+} elevations through PLC-mediated intracellular signaling. These results are in agreement with previous studies that reported that electrophysiological and Ca^{2+} signal effects of ACh on neurons are mediated by PLC activation (Aiken, Lampe, Murphy, & Brown, 1995; Brown & Yu, 2000; Dasari & Gulledge, 2011; Suh & Hille, 2002; Zhang et al., 2003). G_qDREADD activation has also been shown to induce neuronal Ca^{2+} increases (Alexander et al., 2009; Armbruster et al., 2007). Present data further show that G_qDREADD activation also evokes similar electrophysiological responses as ACh, and that the Ca^{2+} elevations are mediated by the PLC signaling pathway. In contrast, we found that endogenous or chemogenetic $G_{i/o}$ GPCR activation elicited neuronal outward currents and hyperpolarizations (Armbruster et al., 2007; Logothetis et al., 1987; North, 1989; Wickman et al., 1994; Zhu et al., 2014), and no Ca^{2+} changes. Regarding Ca^{2+} signaling, the βγ

subunit dissociation after $G_{i/o}$ activation can activate either PLC (Singer, Brown, & Sternweis, 1997) or the IP_3R directly (Zeng et al., 2003), leading to Ca^{2+}mobilization from internal stores. It was interesting that we did not see this increase in neuronal Ca^{2+}, suggesting either that this signaling pathway was not activated, or that we were not able to detect it. This finding contrasts with results from $G_{i/o}$DREADD signaling in astrocytes (see below), where $G_{i/o}$DREADD activation led to Ca^{2+} increases. Taken together, these data are in agreement with and expand upon previous literature showing that $G_{i/o}$ activation is inhibitory in neurons.

In contrast to the differential effects of G_q and $G_{i/o}$ GPCR signaling in neurons, both types of G proteins led to cellular activation in astrocytes in the form of Ca^{2+} increases. Our results show that ACh and G_qDREADD activation similarly increases Ca^{2+} in astrocyte somas and processes through PLC- and IP_3R2-mediated signaling pathways. Our data expand upon existing literature regarding astrocyte responsiveness to ACh (Araque et al., 2002; Chen et al., 2012; Navarrete et al., 2012; Perea & Araque, 2005; Shelton & McCarthy, 2000; Takata et al., 2011). Since previous studies used either a nonselective mAChR antagonist or techniques to manipulate Ca^{2+} release from internal stores, the specific GPCR pathway mediating the Ca^{2+} responses was not known. Here we used PLC and $G_{i/o}$ inhibitors to block G_q- and $G_{i/o}$-mediated effects, respectively. Since $G_{i/o}$ GPCR signaling has also been reported to activate PLC through the $\beta\gamma$ subunit (Singer et al., 1997), U73122 treatment could also block any potential $G_{i/o}$-induced activation of PLC. Additionally, the $\beta\gamma$ subunits that dissociate from $G_{i/o}$ GPCR activation could directly activate the IP_3R (Zeng et al., 2003). Accordingly, there could be residual Ca^{2+} elevation with U73122 treatment alone, due to $\beta\gamma$ activation of the IP_3R, as well as with PTX treatment alone, due to PLC-activated production of IP_3. However, we observed that the ACh-induced Ca^{2+} responses were largely mediated through G_q-PLC-IP_3 than through $G_{i/o}$-$\beta\gamma$-IP_3R2 signaling.

G_qDREADDs have been previously used to specifically activate astrocytes (Adamsky et al., 2018; Agulhon et al., 2013; Bonder & McCarthy, 2014; Bull et al., 2014; Chai et al., 2017; Martin-Fernandez et al., 2017; Scofield et al., 2015), but the Ca^{2+} dynamics and intracellular signaling pathways involved were not fully characterized. We show that G_qDREADD activation stimulated Ca^{2+} increases in a manner akin to endogenous Ca^{2+} dynamics evoked by an endogenous stimulus (i.e., ACh; see Figure 2), and through the canonical signaling of G_q GPCRs, i.e., PLC activation and IP_3-mediated Ca^{2+} mobilization. These results indicate that astrocyte activation via G_qDREADDs closely mimics physiological stimuli.

Unlike in neurons, endogenous and chemogenetic $G_{i/o}$ GPCR signaling led to astrocyte activation in the form of Ca^{2+} increases in a PTX-sensitive manner, demonstrating that the responses were indeed mediated by the $G_{i/o}$ type of G protein. This is in line with other studies showing Ca^{2+} elevations in astrocyte somas upon $G_{i/o}$-coupled $GABA_B$ receptor activation (Covelo & Araque, 2018; Kang et al., 1998; Meier et al., 2008; Navarrete & Araque, 2008; Perea et al., 2016; Serrano, Haddjeri, Lacaille, & Robitaille, 2006). Here, we show $GABA_B$ activation also induces Ca^{2+} increases in astrocytic processes. It seems highly likely that other endogenous neurotransmitters coupled to $G_{i/o}$ GPCRs may also activate astrocytes, but further studies are required to test this hypothesis.

Boddum et al. (2016) have recently reported that activation of astrocyte GABA transporters lead to astrocytic Na^+ concentration elevations and consequent astrocytic Ca^{2+} increases through Na^+/Ca^{2+} exchange (Boddum et al., 2016). Present results indicate that the GABA effects on astrocyte Ca^{2+} are mediated by $GABA_B$ receptor activation because they are blocked by the receptor antagonist CGP. These results are consistent with two different and complementary mechanisms mediated by GABA transporters and receptors that are revealed by different experimental conditions. Indeed, Boddum et al. used long (≥ 5min) bath applications of GABA, which led to astrocytic Na^+ concentration raise, consequent increase in astrocytic Ca^{2+} through Na^+/Ca^{2+} exchange and downstream effects with slow time course (on a temporal scale of minutes). In our study, we used local puff application of GABA (2s) and monitored the short-term effects on astrocyte Ca^{2+} (on a temporal scale of seconds). Therefore, GABA signaling in astrocytes may occur through two complementary mechanisms with different time courses mediated by GABA transporters and receptors.

It has been reported that $GABA_B$ receptor-induced Ca^{2+} elevations can be attributed to PLC signaling (Hirono, Yoshioka, & Konishi, 2001; New, An, Ip, & Wong, 2006) and PTX-sensitive Ca^{2+} mobilization through the IP_3R2 (Mariotti et al., 2016). $G_{i/o}$ GPCR activation can result in PLC-induced Ca^{2+} mobilization through $G_{i/o}$-βγ-PLC signaling (Singer et al., 1997), however, we found no effect of U73122 in GABA- and CNO-induced Ca^{2+} signaling in astrocytes, and instead found that PTX treatment alone abolished the Ca^{2+} increase. Moreover, the lack of CNO-evoked Ca^{2+} increases in $IP_3R2^{-/-}$ mice suggests that both the G_q and $G_{i/o}$ protein-induced Ca^{2+} increases require IP_3R2 activation. These data suggest that $G_{i/o}$GPCR-induced Ca^{2+} elevations in astrocytes may have been mediated via βγ subunits directly binding the IP_3R2 (Zeng et al., 2003) and not through PLC activation. Future experiments, for example using βγ inhibitors, are necessary to determine the specific signaling cascade leading to Ca^{2+} elevations. Taken together, both GPCR pathways appear to converge on the IP_3R2, but differ in the exact signaling mechanisms leading to IP_3R2 activation. Lastly, we found *in vivo* that activation of either G_q or $G_{i/o}$ DREADDs targeted to cortical astrocytes induced an increase in Ca^{2+} events following CNO injection. These data provide evidence that this chemogenetic approach to selectively activate astrocytes remains feasible in a more intact preparation.

Both G_q- and $G_{i/o}$-induced astrocyte Ca^{2+} elevations, whether elicited by endogenous receptors or DREADDs, stimulated glutamate release from astrocytes, which was detected as an increase in the frequency of SICs. SICs, which are known to be mediated by activation of neuronal NMDA receptors, have been found to enhance neuronal excitability and increase neuronal synchrony (Angulo et al., 2004; Araque, Sanzgiri, et al., 1998; Fellin et al., 2004; Perea & Araque, 2005; Shigetomi, Bowser, Sofroniew, & Khakh, 2008). While a recent study using G_qDREADDs in astrocytes failed to detect significant changes in SIC frequency upon CNO stimulation (Chai et al., 2017), we observed robust effects. Although the origin of these discrepant results is unclear, it may be due to different sensitivity in detecting SICs, as indicated by our relatively lower mean SIC amplitude.

In addition to an increase in SIC frequency in nearby neurons, selective astrocyte activation via either G_qDREADD or $G_{i/o}$DREADD signaling led to an increase in action potential firing of hippocampal neurons. While most reports of neuronal-glial interactions have shown

synaptic transmission regulation by astrocytes (Araque et al., 2014), present results add to recent studies showing that astrocytes can also regulate neuronal firing and network activity (Lee et al., 2014; Poskanzer & Yuste, 2011, 2016; Shen, Nikolic, Meunier, Pfrieger, & Audinat, 2017; Tan et al., 2017). Indeed, the observed increase in astrocyte Ca^{2+} activity upon CNO injection *in vivo* co-occurred with an upregulated delta range of the slow-wave activity. This is consistent with previous studies showing the contribution of gliotransmission to *in vivo* network function (Fellin et al., 2009; Poskanzer & Yuste, 2011). Interestingly, our findings show that stimulating either the G_q or $G_{i/o}$ protein pathways in astrocytes led to increases in astrocyte Ca^{2+} and slow-wave activity in the delta range *in vivo*, suggesting both pathways play similar regulatory roles in the living brain. The absence of effects of CNO administration in slice and *in vivo* in mice injected with the control virus AAV8-GFAP-mCherry indicates that the observed effects of CNO are not due to off-target effects but rather direct activation of astrocytes. It is important to note that mechanistic correlations should not be made between the results obtained *in situ* with those obtained *in vivo*, as these two regions have distinct neuronal-glial network interactions. Rather, we aimed to expand our results *in vivo* to test the hypothesis that activating astrocytes either via G_q or $G_{i/o}$ protein signaling pathways influenced neuronal network activity. Taken together, astrocytes have multiple modulatory roles, controlling neuronal information processing via synaptic transmission as well as directly regulating neuronal output and network activity.

The excitation/inhibition balance is important for proper brain function, and its dysfunction may lead to brain disorders, such as epilepsy and autism. In addition to the importance of excitatory transmission in brain communication, inhibitory transmission controls synaptic transmission and neuronal firing frequency (Buzsaki & Chrobak, 1995; Engel et al., 2001; Salinas & Sejnowski, 2001). Beyond the direct effects on cell signaling reduction, inhibition is essential in the operation of neural networks, contributing to the generation of rhythmic activity by synchronizing the discharge of principal cell populations (Bartos, Vida, & Jonas, 2007; Kullmann, 2011; Pouille & Scanziani, 2001). Present findings indicate that inhibition is a specific property of neurons and may be fundamentally different between neurons and astrocytes. While inhibitory neurotransmitters have direct inhibitory effects on neuronal activity through direct activation of neuronal receptors, present data indicate that they may also have an indirect excitatory effect on neurons through activation of astrocytes. Hence, the same neurotransmitters that directly inhibit neurons may also activate astrocytes, which then feed-forward excite neurons (Perea et al., 2016). Therefore, the present results reveal additional complexity of the signaling consequences of excitatory and inhibitory neurotransmitters in network operation and brain function.

Acknowledgements

We would like to thank Ruth Quintana, Stephanie Nistler, and Heidi Busch for technical support; Mario Martin, and Michelle Corkrum for helpful suggestions; Mark Sanders, Guillermo Marques and Jason Mitchell at the University of Minnesota – University Imaging Centers for assistance using the Leica SP5 Multiphoton Confocal Upright Microscope; The MnDRIVE Optogenetics Core at the University of Minnesota for technical support; Viral vectors used in this study were prepared by the University of Minnesota Viral Vector and Cloning Core; Ju Chen for generously donating the $IP_3R2^{-/-}$ mice; Dwight Bergles and Amit Agarwal for generously donating the GLAST-CreERT2xR26-lsl-GCaMP3 mice; and the UNC Vector Core for providing the DREADDs viruses. This work was supported by NIH-NINDS (R01NS097312–01) and Human Frontier Science Program (Research Grant RGP0036/2014) to A.A and NIH-NINDS (5 F31 NS 93751–3) to C.A.D and NIH-NIA (1 F31 AG057155–01A1) to J.L.. The authors declare no competing financial interests.

REFERENCES

Adamsky A, Kol A, Kreisel T, Doron A, Ozeri-Engelhard N, Melcer T, . . . Goshen I (2018). Astrocytic Activation Generates De Novo Neuronal Potentiation and Memory Enhancement. Cell. doi:10.1016/j.cell.2018.05.002

Agarwal A, Wu PH, Hughes EG, Fukaya M, Tischfield MA, Langseth AJ, . . . Bergles DE (2017). Transient Opening of the Mitochondrial Permeability Transition Pore Induces Microdomain Calcium Transients in Astrocyte Processes. Neuron, 93(3), 587-605 e587. doi:10.1016/j.neuron.2016.12.034 [PubMed: 28132831]

Agulhon C, Boyt KM, Xie AX, Friocourt F, Roth BL, & McCarthy KD (2013). Modulation of the autonomic nervous system and behaviour by acute glial cell Gq protein-coupled receptor activation in vivo. J Physiol, 591(22), 5599–5609. doi:10.1113/jphysiol.2013.261289 [PubMed: 24042499]

Aiken SP, Lampe BJ, Murphy PA, & Brown BS (1995). Reduction of spike frequency adaptation and blockade of M-current in rat CA1 pyramidal neurones by linopirdine (DuP 996), a neurotransmitter release enhancer. Br J Pharmacol, 115(7), 1163–1168. [PubMed: 7582539]

Alexander GM, Rogan SC, Abbas AI, Armbruster BN, Pei Y, Allen JA, . . . Roth BL. (2009). Remote control of neuronal activity in transgenic mice expressing evolved G protein-coupled receptors. Neuron, 63(1), 27–39. doi:10.1016/j.neuron.2009.06.014 [PubMed: 19607790]

Angulo MC, Kozlov AS, Charpak S, & Audinat E (2004). Glutamate released from glial cells synchronizes neuronal activity in the hippocampus. J Neurosci, 24(31), 6920–6927. doi:10.1523/JNEUROSCI.0473-04.2004 [PubMed: 15295027]

Araque A, Carmignoto G, & Haydon PG (2001). Dynamic signaling between astrocytes and neurons. Annu Rev Physiol, 63, 795–813. doi:10.1146/annurev.physiol.63.1.795 [PubMed: 11181976]

Araque A, Carmignoto G, Haydon PG, Oliet SH, Robitaille R, & Volterra A (2014). Gliotransmitters travel in time and space. Neuron, 81(4), 728–739. doi:10.1016/j.neuron.2014.02.007 [PubMed: 24559669]

Araque A, Martin ED, Perea G, Arellano JI, & Buno W (2002). Synaptically released acetylcholine evokes Ca2+ elevations in astrocytes in hippocampal slices. J Neurosci, 22(7), 2443–2450. doi: 20026212 [PubMed: 11923408]

Araque A, Parpura V, Sanzgiri RP, & Haydon PG (1998). Glutamate-dependent astrocyte modulation of synaptic transmission between cultured hippocampal neurons. Eur J Neurosci, 10(6), 2129–2142. [PubMed: 9753099]

Araque A, Parpura V, Sanzgiri RP, & Haydon PG (1999). Tripartite synapses: glia, the unacknowledged partner. Trends Neurosci, 22(5), 208–215. [PubMed: 10322493]

Araque A, Sanzgiri RP, Parpura V, & Haydon PG (1998). Calcium elevation in astrocytes causes an NMDA receptor-dependent increase in the frequency of miniature synaptic currents in cultured hippocampal neurons. J Neurosci, 18(17), 6822–6829. [PubMed: 9712653]

Armbruster BN, Li X, Pausch MH, Herlitze S, & Roth BL (2007). Evolving the lock to fit the key to create a family of G protein-coupled receptors potently activated by an inert ligand. Proc Natl Acad Sci U S A, 104(12), 5163–5168. doi:10.1073/pnas.0700293104 [PubMed: 17360345]

Bartos M, Vida I, & Jonas P (2007). Synaptic mechanisms of synchronized gamma oscillations in inhibitory interneuron networks. Nat Rev Neurosci, 8(1), 45–56. doi:10.1038/nrn2044 [PubMed: 17180162]

Berkeley JL, Gomeza J, Wess J, Hamilton SE, Nathanson NM, & Levey AI (2001). M1 muscarinic acetylcholine receptors activate extracellular signal-regulated kinase in CA1 pyramidal neurons in mouse hippocampal slices. Mol Cell Neurosci, 18(5), 512–524. doi:10.1006/mcne.2001.1042 [PubMed: 11922142]

Bezzi P, Gundersen V, Galbete JL, Seifert G, Steinhauser C, Pilati E, & Volterra A (2004). Astrocytes contain a vesicular compartment that is competent for regulated exocytosis of glutamate. Nat Neurosci, 7(6), 613–620. doi:10.1038/nn1246 [PubMed: 15156145]

Boddum K, Jensen TP, Magloire V, Kristiansen U, Rusakov DA, Pavlov I, & Walker MC (2016). Astrocytic GABA transporter activity modulates excitatory neurotransmission. Nat Commun, 7, 13572. doi:10.1038/ncomms13572 [PubMed: 27886179]

Bonder DE, & McCarthy KD (2014). Astrocytic Gq-GPCR-linked IP3R-dependent Ca2+ signaling does not mediate neurovascular coupling in mouse visual cortex in vivo. J Neurosci, 34(39), 13139–13150. doi:10.1523/JNEUROSCI.2591-14.2014 [PubMed: 25253859]

Brown BS, & Yu SP (2000). Modulation and genetic identification of the M channel. Prog Biophys Mol Biol, 73(2–4), 135–166. [PubMed: 10958929]

Bull C, Freitas KC, Zou S, Poland RS, Syed WA, Urban DJ, . . . Bowers MS (2014). Rat nucleus accumbens core astrocytes modulate reward and the motivation to self-administer ethanol after abstinence. Neuropsychopharmacology, 39(12), 2835–2845. doi:10.1038/npp.2014.135 [PubMed: 24903651]

Buzsaki G, & Chrobak JJ (1995). Temporal structure in spatially organized neuronal ensembles: a role for interneuronal networks. Curr Opin Neurobiol, 5(4), 504–510. [PubMed: 7488853]

Chai H, Diaz-Castro B, Shigetomi E, Monte E, Octeau JC, Yu X, . . . Khakh BS (2017). Neural Circuit-Specialized Astrocytes: Transcriptomic, Proteomic, Morphological, and Functional Evidence. Neuron, 95(3), 531-549 e539. doi:10.1016/j.neuron.2017.06.029 [PubMed: 28712653]

Chen N, Sugihara H, Sharma J, Perea G, Petravicz J, Le C, & Sur M (2012). Nucleus basalis-enabled stimulus-specific plasticity in the visual cortex is mediated by astrocytes. Proc Natl Acad Sci U S A, 109(41), E2832–2841. doi:10.1073/pnas.1206557109 [PubMed: 23012414]

Covelo A, & Araque A (2018). Neuronal activity determines distinct gliotransmitter release from a single astrocyte. Elife, 7. doi:10.7554/eLife.32237

Dasari S, & Gulledge AT (2011). M1 and M4 receptors modulate hippocampal pyramidal neurons. J Neurophysiol, 105(2), 779–792. doi:10.1152/jn.00686.2010 [PubMed: 21160001]

Di Castro MA, Chuquet J, Liaudet N, Bhaukaurally K, Santello M, Bouvier D, . . . Volterra A. (2011). Local Ca2+ detection and modulation of synaptic release by astrocytes. Nat Neurosci, 14(10), 1276–1284. doi:10.1038/nn.2929 [PubMed: 21909085]

Engel D, Pahner I, Schulze K, Frahm C, Jarry H, Ahnert-Hilger G, & Draguhn A (2001). Plasticity of rat central inhibitory synapses through GABA metabolism. J Physiol, 535(Pt 2), 473–482. [PubMed: 11533137]

Erondu NE, & Kennedy MB (1985). Regional distribution of type II Ca2+/calmodulin-dependent protein kinase in rat brain. J Neurosci, 5(12), 3270–3277. [PubMed: 4078628]

Fellin T, Halassa MM, Terunuma M, Succol F, Takano H, Frank M, . . . Haydon PG. (2009). Endogenous nonneuronal modulators of synaptic transmission control cortical slow oscillations in vivo. Proc Natl Acad Sci U S A, 106(35), 15037–15042. doi:10.1073/pnas.0906419106 [PubMed: 19706442]

Fellin T, Pascual O, Gobbo S, Pozzan T, Haydon PG, & Carmignoto G (2004). Neuronal synchrony mediated by astrocytic glutamate through activation of extrasynaptic NMDA receptors. Neuron, 43(5), 729–743. doi:10.1016/j.neuron.2004.08.011 [PubMed: 15339653]

Fiacco TA, & McCarthy KD (2018). Multiple Lines of Evidence Indicate That Gliotransmission Does Not Occur under Physiological Conditions. J Neurosci, 38(1), 3–13. doi:10.1523/JNEUROSCI.0016-17.2017 [PubMed: 29298904]

Gasparini S, & Magee JC (2006). State-dependent dendritic computation in hippocampal CA1 pyramidal neurons. J Neurosci, 26(7), 2088–2100. doi:10.1523/JNEUROSCI.4428-05.2006 [PubMed: 16481442]

Gomez-Gonzalo M, Navarrete M, Perea G, Covelo A, Martin-Fernandez M, Shigemoto R, . . . Araque A. (2015). Endocannabinoids Induce Lateral Long-Term Potentiation of Transmitter Release by Stimulation of Gliotransmission. Cereb Cortex, 25(10), 3699–3712. doi:10.1093/cercor/bhu231 [PubMed: 25260706]

Halassa MM, & Haydon PG (2010). Integrated brain circuits: astrocytic networks modulate neuronal activity and behavior. Annu Rev Physiol, 72, 335–355. doi:10.1146/annurev-physiol-021909-135843 [PubMed: 20148679]

Haydon PG, & Carmignoto G (2006). Astrocyte control of synaptic transmission and neurovascular coupling. Physiol Rev, 86(3), 1009–1031. doi:10.1152/physrev.00049.2005 [PubMed: 16816144]

Hirono M, Yoshioka T, & Konishi S (2001). GABA(B) receptor activation enhances mGluR-mediated responses at cerebellar excitatory synapses. Nat Neurosci, 4(12), 1207–1216. doi:10.1038/nn764

Huang Y, & Thathiah A (2015). Regulation of neuronal communication by G protein-coupled receptors. FEBS Lett, 589(14), 1607–1619. doi:10.1016/j.febslet.2015.05.007 [PubMed: 25980603]

Kang J, Jiang L, Goldman SA, & Nedergaard M (1998). Astrocyte-mediated potentiation of inhibitory synaptic transmission. Nat Neurosci, 1(8), 683–692. doi:10.1038/3684 [PubMed: 10196584]

Kullmann DM (2011). Interneuron networks in the hippocampus. Curr Opin Neurobiol, 21(5), 709–716. doi:10.1016/j.conb.2011.05.006 [PubMed: 21636266]

Lauckner JE, Hille B, & Mackie K (2005). The cannabinoid agonist WIN55,212–2 increases intracellular calcium via CB1 receptor coupling to Gq/11 G proteins. Proc Natl Acad Sci U S A, 102(52), 19144–19149. doi:10.1073/pnas.0509588102 [PubMed: 16365309]

Lee HS, Ghetti A, Pinto-Duarte A, Wang X, Dziewczapolski G, Galimi F, . . . Heinemann SF. (2014). Astrocytes contribute to gamma oscillations and recognition memory. Proc Natl Acad Sci U S A, 111(32), E3343–3352. doi:10.1073/pnas.1410893111 [PubMed: 25071179]

Li X, Zima AV, Sheikh F, Blatter LA, & Chen J (2005). Endothelin-1-induced arrhythmogenic Ca2+ signaling is abolished in atrial myocytes of inositol-1,4,5-trisphosphate(IP3)-receptor type 2-deficient mice. Circ Res, 96(12), 1274–1281. doi:10.1161/01.RES.0000172556.05576.4c [PubMed: 15933266]

Logothetis DE, Kurachi Y, Galper J, Neer EJ, & Clapham DE (1987). The beta gamma subunits of GTP-binding proteins activate the muscarinic K+ channel in heart. Nature, 325(6102), 321–326. doi:10.1038/325321a0 [PubMed: 2433589]

Magee JC, & Carruth M (1999). Dendritic voltage-gated ion channels regulate the action potential firing mode of hippocampal CA1 pyramidal neurons. J Neurophysiol, 82(4), 1895–1901. [PubMed: 10515978]

Mariotti L, Losi G, Lia A, Melone M, Chiavegato A, Gomez-Gonzalo M, . . . Carmignoto G (2018). Interneuron-specific signaling evokes distinctive somatostatin-mediated responses in adult cortical astrocytes. Nat Commun, 9(1), 82. doi:10.1038/s41467-017-02642-6 [PubMed: 29311610]

Mariotti L, Losi G, Sessolo M, Marcon I, & Carmignoto G (2016). The inhibitory neurotransmitter GABA evokes long-lasting Ca(2+) oscillations in cortical astrocytes. Glia, 64(3), 363–373. doi:10.1002/glia.22933 [PubMed: 26496414]

Martin-Fernandez M, Jamison S, Robin LM, Zhao Z, Martin ED, Aguilar J, . . . Araque A (2017). Synapse-specific astrocyte gating of amygdala-related behavior. Nat Neurosci, 20(11), 1540–1548. doi:10.1038/nn.4649 [PubMed: 28945222]

Martin R, Bajo-Graneras R, Moratalla R, Perea G, & Araque A (2015). Circuit-specific signaling in astrocyte-neuron networks in basal ganglia pathways. Science, 349(6249), 730–734. doi:10.1126/science.aaa7945 [PubMed: 26273054]

Meier SD, Kafitz KW, & Rose CR (2008). Developmental profile and mechanisms of GABA-induced calcium signaling in hippocampal astrocytes. Glia, 56(10), 1127–1137. doi:10.1002/glia.20684 [PubMed: 18442094]

Navarrete M, & Araque A (2008). Endocannabinoids mediate neuron-astrocyte communication. Neuron, 57(6), 883–893. doi:10.1016/j.neuron.2008.01.029 [PubMed: 18367089]

Navarrete M, & Araque A (2010). Endocannabinoids potentiate synaptic transmission through stimulation of astrocytes. Neuron, 68(1), 113–126. doi:10.1016/j.neuron.2010.08.043 [PubMed: 20920795]

Navarrete M, Perea G, Fernandez de Sevilla D, Gomez-Gonzalo M, Nunez A, Martin ED, & Araque A (2012). Astrocytes mediate in vivo cholinergic-induced synaptic plasticity. PLoS Biol, 10(2), e1001259. doi:10.1371/journal.pbio.1001259 [PubMed: 22347811]

New DC, An H, Ip NY, & Wong YH (2006). GABAB heterodimeric receptors promote Ca2+ influx via store-operated channels in rat cortical neurons and transfected Chinese hamster ovary cells. Neuroscience, 137(4), 1347–1358. doi:10.1016/j.neuroscience.2005.10.033 [PubMed: 16343781]

North RA (1989). Twelfth Gaddum memorial lecture. Drug receptors and the inhibition of nerve cells. Br J Pharmacol, 98(1), 13–28. [PubMed: 2679954]

Panatier A, Vallee J, Haber M, Murai KK, Lacaille JC, & Robitaille R (2011). Astrocytes are endogenous regulators of basal transmission at central synapses. Cell, 146(5), 785–798. doi:10.1016/j.cell.2011.07.022 [PubMed: 21855979]

Park JY, & Spruston N (2012). Synergistic actions of metabotropic acetylcholine and glutamate receptors on the excitability of hippocampal CA1 pyramidal neurons. J Neurosci, 32(18), 6081–6091. doi:10.1523/JNEUROSCI.6519-11.2012 [PubMed: 22553015]

Pasti L, Volterra A, Pozzan T, & Carmignoto G (1997). Intracellular calcium oscillations in astrocytes: a highly plastic, bidirectional form of communication between neurons and astrocytes in situ. J Neurosci, 17(20), 7817–7830. [PubMed: 9315902]

Paukert M, Agarwal A, Cha J, Doze VA, Kang JU, & Bergles DE (2014). Norepinephrine controls astroglial responsiveness to local circuit activity. Neuron, 82(6), 1263–1270. doi:10.1016/j.neuron.2014.04.038 [PubMed: 24945771]

Perea G, & Araque A (2005). Properties of synaptically evoked astrocyte calcium signal reveal synaptic information processing by astrocytes. J Neurosci, 25(9), 2192–2203. doi:10.1523/JNEUROSCI.3965-04.2005 [PubMed: 15745945]

Perea G, Gomez R, Mederos S, Covelo A, Ballesteros JJ, Schlosser L, ...Araque A (2016). Activity-dependent switch of GABAergic inhibition into glutamatergic excitation in astrocyte-neuron networks. Elife, 5. doi:10.7554/eLife.20362

Perea G, Navarrete M, & Araque A (2009). Tripartite synapses: astrocytes process and control synaptic information. Trends Neurosci, 32(8), 421–431. doi:10.1016/j.tins.2009.05.001 [PubMed: 19615761]

Perea G, Sur M, & Araque A (2014). Neuron-glia networks: integral gear of brain function. Front Cell Neurosci, 8, 378. doi:10.3389/fncel.2014.00378 [PubMed: 25414643]

Petravicz J, Fiacco TA, & McCarthy KD (2008). Loss of IP3 receptor-dependent Ca2+ increases in hippocampal astrocytes does not affect baseline CA1 pyramidal neuron synaptic activity. J Neurosci, 28(19), 4967–4973. doi:10.1523/JNEUROSCI.5572-07.2008 [PubMed: 18463250]

Porter JT, & McCarthy KD (1996). Hippocampal astrocytes in situ respond to glutamate released from synaptic terminals. J Neurosci, 16(16), 5073–5081. [PubMed: 8756437]

Poskanzer KE, & Yuste R (2011). Astrocytic regulation of cortical UP states. Proc Natl Acad Sci U S A, 108(45), 18453–18458. doi:10.1073/pnas.1112378108 [PubMed: 22027012]

Poskanzer KE, & Yuste R (2016). Astrocytes regulate cortical state switching in vivo. Proc Natl Acad Sci U S A, 113(19), E2675–2684. doi:10.1073/pnas.1520759113 [PubMed: 27122314]

Pouille F, & Scanziani M (2001). Enforcement of temporal fidelity in pyramidal cells by somatic feed-forward inhibition. Science, 293(5532), 1159–1163. doi:10.1126/science.1060342 [PubMed: 11498596]

Rusakov DA (2015). Disentangling calcium-driven astrocyte physiology. Nat Rev Neurosci, 16(4), 226–233. doi:10.1038/nrn3878 [PubMed: 25757560]

Salinas E, & Sejnowski TJ (2001). Correlated neuronal activity and the flow of neural information. Nat Rev Neurosci, 2(8), 539–550. doi:10.1038/35086012 [PubMed: 11483997]

Scheiderer CL, Smith CC, McCutchen E, McCoy PA, Thacker EE, Kolasa K, . . . McMahon LL. (2008). Coactivation of M(1) muscarinic and alpha1 adrenergic receptors stimulates extracellular signal-regulated protein kinase and induces long-term depression at CA3-CA1 synapses in rat hippocampus. J Neurosci, 28(20), 5350–5358. doi:10.1523/JNEUROSCI.5058-06.2008 [PubMed: 18480291]

Schulman H, & Lou LL (1989). Multifunctional Ca2+/calmodulin-dependent protein kinase: domain structure and regulation. Trends Biochem Sci, 14(2), 62–66. [PubMed: 2539662]

Scofield MD, Boger HA, Smith RJ, Li H, Haydon PG, & Kalivas PW (2015). Gq-DREADD Selectively Initiates Glial Glutamate Release and Inhibits Cue-induced Cocaine Seeking. Biol Psychiatry, 78(7), 441–451. doi:10.1016/j.biopsych.2015.02.016 [PubMed: 25861696]

Serrano A, Haddjeri N, Lacaille JC, & Robitaille R (2006). GABAergic network activation of glial cells underlies hippocampal heterosynaptic depression. J Neurosci, 26(20), 5370–5382. doi:10.1523/JNEUROSCI.5255-05.2006 [PubMed: 16707789]

Shelton MK, & McCarthy KD (2000). Hippocampal astrocytes exhibit Ca2+-elevating muscarinic cholinergic and histaminergic receptors in situ. J Neurochem, 74(2), 555–563. [PubMed: 10646506]

Shen W, Nikolic L, Meunier C, Pfrieger F, & Audinat E (2017). An autocrine purinergic signaling controls astrocyte-induced neuronal excitation. Sci Rep, 7(1), 11280. doi:10.1038/s41598-017-11793-x [PubMed: 28900295]

Shigetomi E, Bowser DN, Sofroniew MV, & Khakh BS (2008). Two forms of astrocyte calcium excitability have distinct effects on NMDA receptor-mediated slow inward currents in pyramidal neurons. J Neurosci, 28(26), 6659–6663. doi:10.1523/JNEUROSCI.1717-08.2008 [PubMed: 18579739]

Singer WD, Brown HA, & Sternweis PC (1997). Regulation of eukaryotic phosphatidylinositol-specific phospholipase C and phospholipase D. Annu Rev Biochem, 66, 475–509. doi:10.1146/annurev.biochem.66.1.475 [PubMed: 9242915]

Stewart A, & Fisher RA (2015). Introduction: G Protein-coupled Receptors and RGS Proteins. Prog Mol Biol Transl Sci, 133, 1–11. doi:10.1016/bs.pmbts.2015.03.002 [PubMed: 26123299]

Suh BC, & Hille B (2002). Recovery from muscarinic modulation of M current channels requires phosphatidylinositol 4,5-bisphosphate synthesis. Neuron, 35(3), 507–520. [PubMed: 12165472]

Takata N, Mishima T, Hisatsune C, Nagai T, Ebisui E, Mikoshiba K, & Hirase H (2011). Astrocyte calcium signaling transforms cholinergic modulation to cortical plasticity in vivo. J Neurosci, 31(49), 18155–18165. doi:10.1523/JNEUROSCI.5289-11.2011 [PubMed: 22159127]

Tan Z, Liu Y, Xi W, Lou HF, Zhu L, Guo Z, ...Duan S. (2017). Glia-derived ATP inversely regulates excitability of pyramidal and CCK-positive neurons. Nat Commun, 8, 13772. doi:10.1038/ncomms13772 [PubMed: 28128211]

Verkhratsky A, & Kettenmann H (1996). Calcium signalling in glial cells. Trends Neurosci, 19(8), 346–352. [PubMed: 8843604]

Volterra A, Liaudet N, & Savtchouk I (2014). Astrocyte Ca(2)(+) signalling: an unexpected complexity. Nat Rev Neurosci, 15(5), 327–335. doi:10.1038/nrn3725 [PubMed: 24739787]

Volterra A, & Meldolesi J (2005). Astrocytes, from brain glue to communication elements: the revolution continues. Nat Rev Neurosci, 6(8), 626–640. doi:10.1038/nrn1722 [PubMed: 16025096]

Wickman KD, Iniguez-Lluhl JA, Davenport PA, Taussig R, Krapivinsky GB, Linder ME, . . . Clapham DE (1994). Recombinant G-protein beta gamma-subunits activate the muscarinic-gated atrial potassium channel. Nature, 368(6468), 255–257. doi:10.1038/368255a0 [PubMed: 8145826]

Zeng W, Mak DO, Li Q, Shin DM, Foskett JK, & Muallem S (2003). A new mode of Ca2+ signaling by G protein-coupled receptors: gating of IP3 receptor Ca2+ release channels by Gbetagamma. Curr Biol, 13(10), 872–876. [PubMed: 12747838]

Zhang H, Craciun LC, Mirshahi T, Rohacs T, Lopes CM, Jin T, & Logothetis DE (2003). PIP(2) activates KCNQ channels, and its hydrolysis underlies receptor-mediated inhibition of M currents. Neuron, 37(6), 963–975. [PubMed: 12670425]

Zhu H, Pleil KE, Urban DJ, Moy SS, Kash TL, & Roth BL (2014). Chemogenetic inactivation of ventral hippocampal glutamatergic neurons disrupts consolidation of contextual fear memory. Neuropsychopharmacology, 39(8), 1880–1892. doi:10.1038/npp.2014.35 [PubMed: 24525710]

Main points

G_q signaling in neurons and astrocytes leads to cellular activation, but while $G_{i/o}$ signaling in neurons leads to cellular inhibition, it leads to activation in astrocytes and downstream gliotransmission that modulates neuronal activity.

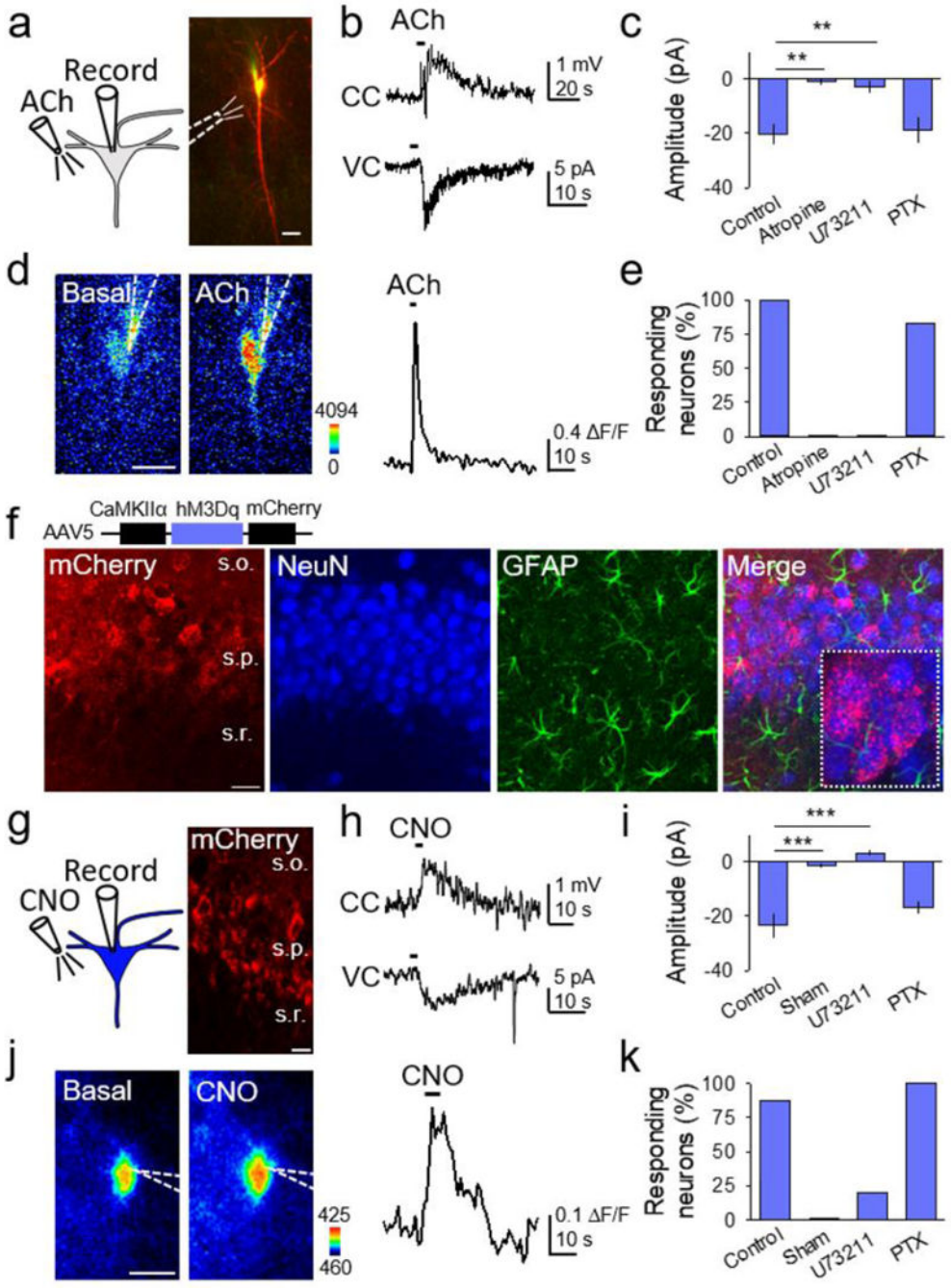

Figure 1. G_q signaling induces neuronal activation.

(A) Scheme of neuronal G_q GPCR activation by ACh, and TexasRed and Fluo4-filled CA1 neuron (scale bar, 20μm). (B) Representative traces showing effects of local ACh application in current clamp (CC) and voltage clamp (VC). (C) ACh-induced current amplitude in different conditions (Kruskal-Wallis One-way ANOVA, $p < 0.001$). (D) Pseudocolor Fluo4 fluorescence images before and after ACh application in the neuron depicted in (A) (scale bar, 20μm), and corresponding fluorescent Ca^{2+} trace. (E) Percentage of neurons that responded with a Ca^{2+} increase to ACh in different conditions. (F) Immunohistochemical

images of hippocampus injected with AAV5-CaMKIIα-hM3Dq-mCherry. *From left to right*: mCherry, NeuN, GFAP and merge (scale bar, 25 μm; s.o., stratum oriens; s.p., stratum pyramidale; s.r., stratum radiatum). (G) Scheme of neuronal chemogenetic G_qDREADD activation and image showing mCherry-expressing CA1 neurons (scale bar, 15 μm). (H) Representative traces showing effects of local CNO application in CC and VC. (I) CNO-induced current amplitude in different conditions (Kruskal-Wallis One-way ANOVA, $p < 0.001$). (J) Pseudocolor Fluo4 fluorescence image before and after CNO application (scale bar, 10μm), and corresponding fluorescent Ca^{2+} trace. (K) Percentage of neurons that responded with a Ca^{2+} increase to CNO in different conditions. Data are represented as mean ± SEM. $P < 0.01$ (**), and $P < 0.001$ (***).

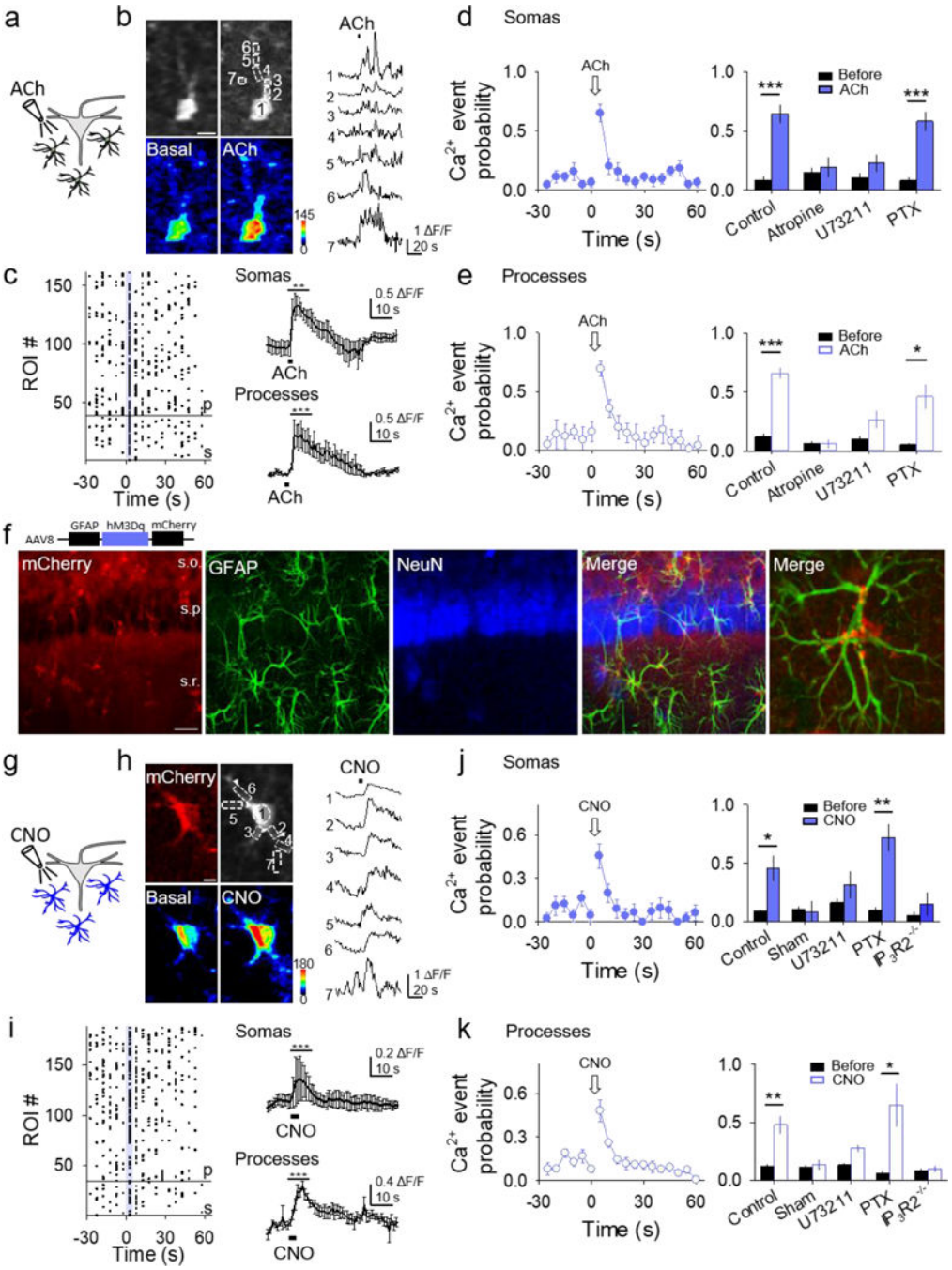

Figure 2. G_q activation in astrocytes elevates their Ca2+ levels.

(A) Scheme of G_q GPCR activation in astrocytes by ACh locally applied over *stratum radiatum* astrocytes. (B) Fluorescence images of an astrocyte showing selected domains in soma and processes (*top*), pseudocolor Ca^{2+} images before (basal) and after local application of ACh (*bottom*) (scale bar, 5 μm), and Ca^{2+} traces from domains shown in top right panel. (C) *Left:* Raster plot showing Ca^{2+} events for each ROI (somas (s) below reference line, processes (p) above reference line). *Right:* Average Ca^{2+} traces from responding somas (*top*) and processes (*bottom*). T-test compares 10s before and 10s after

agonist. (D and E) Ca^{2+} event probability in somas (D) and processes (E) *vs.* time, and maximum values in different conditions. (F) Immunohistochemical images of AAV8-GFAP-hM3Dq-mCherry expression in the hippocampus. *From left to right*: Expression of mCherry, GFAP, NeuN, a merge of all three, and a higher magnification merge image showing colocalization of GFAP and mCherry (25x; scale bar, 20 μm; s.o., stratum oriens; s.p., stratum pyramidale; s.r., stratum radiatum). (G-K) as (A-E) but with local application of CNO to G_qDREADD expressing astrocytes instead of ACh. Data are represented as mean ± SEM. $P < 0.05$ (*), $P < 0.01$ (**), and $P < 0.001$ (***).

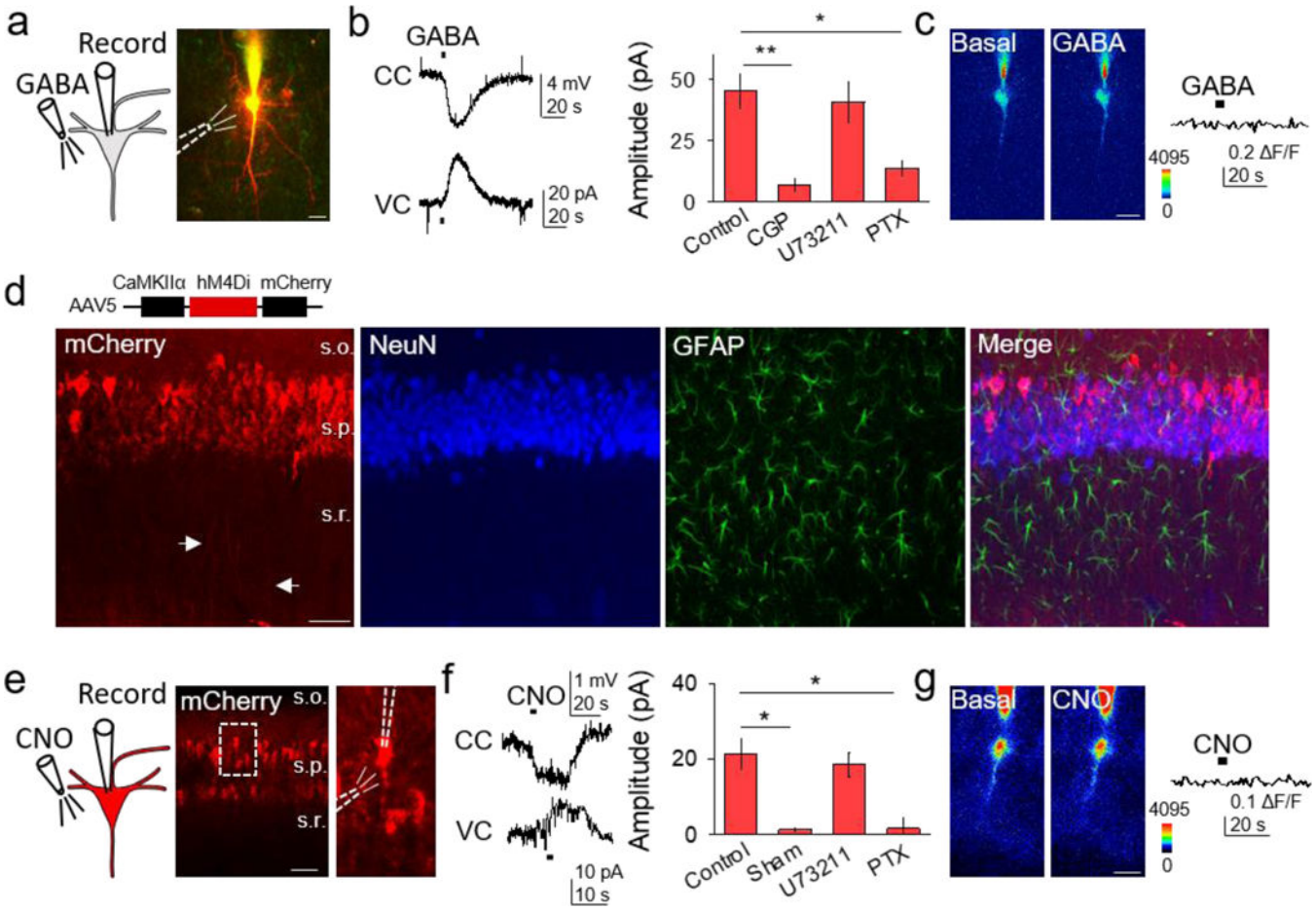

Figure 3. $G_{i/o}$ activation in neurons is inhibitory.

(A) Scheme of neuronal $G_{i/o}$ activation by GABA, and TexasRed and Fluo4-filled CA1 neuron (scale bar, 20μm). (B) Representative traces showing GABA-induced responses in current clamp (CC) and voltage clamp (VC), and GABA-induced current amplitude in different conditions (Kruskal-Wallis One-way ANOVA, $p < 0.01$, $p < 0.05$). (C) Pseudocolor Fluo4 images before and after GABA application from the neuron depicted in (A) (scale bar, 20μm), and the corresponding fluorescent Ca^{2+} trace. (D) Immunohistochemical images of AAV5-CaMKIIα-hM4Di-mCherry expression in hippocampus. *From left to right*: mCherry, NeuN, GFAP and merge (scale bar, 50 μm; s.o., stratum oriens; s.p., stratum pyramidale; s.r., stratum radiatum). (E) Scheme of neuronal chemogenetic $G_{i/o}$DREADD activation and fluorescent image showing mCherry-expressing neurons (scale bar, 50μm). (F) Representative traces showing CNO-evoked responses in CC and VC, and CNO-induced current amplitude in different conditions (Kruskal-Wallis One-way ANOVA, $p < 0.05$). (G) Pseudocolor Fluo4 images before and after CNO application (scale bar, 20μm), and corresponding fluorescent Ca^{2+} trace. Data are represented as mean ± SEM. $P < 0.05$ (*) and $P < 0.01$ (**).

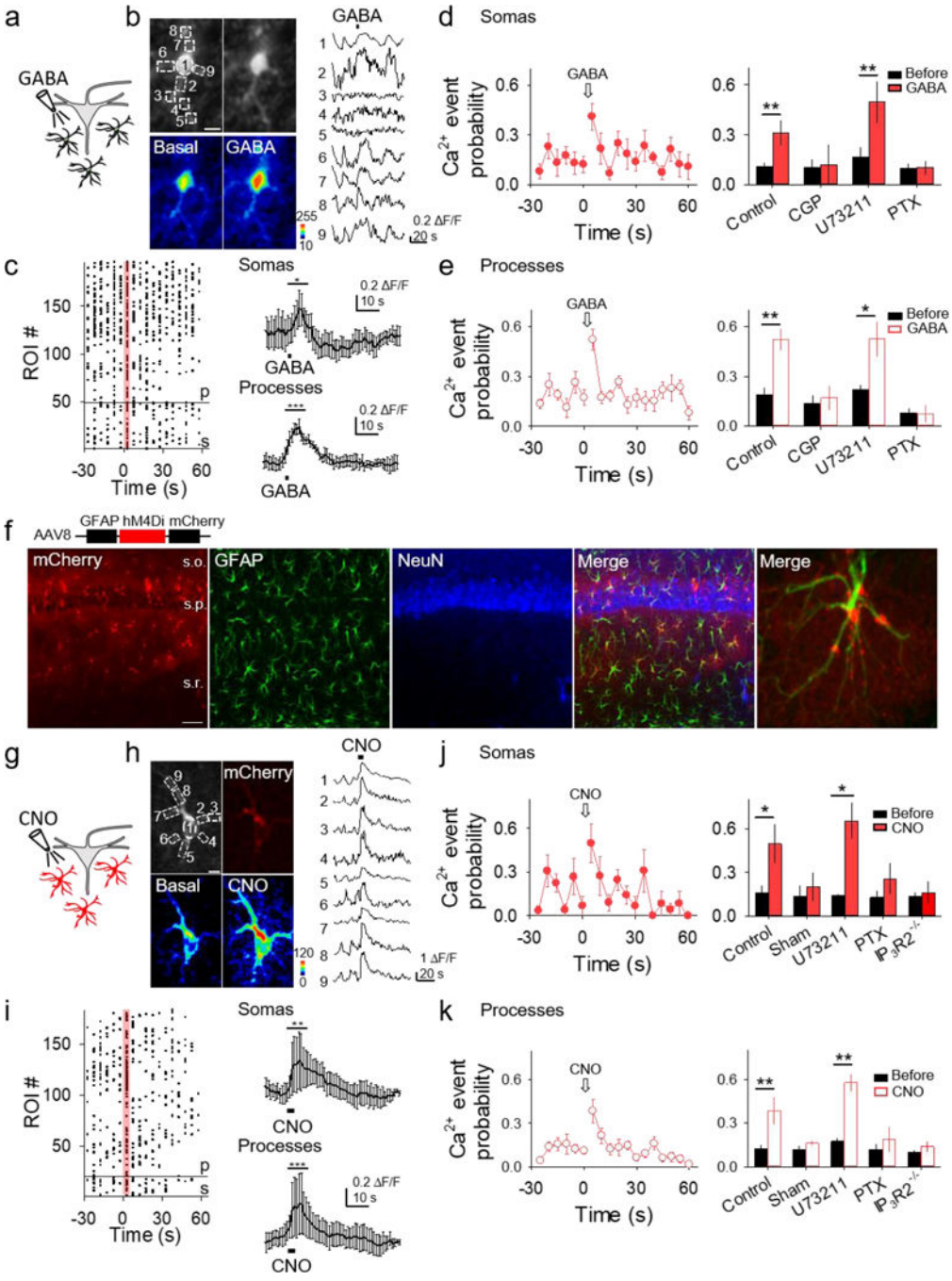

Figure 4. $G_{i/o}$ activation in astrocytes elevates their Ca2+ levels.

(A) Scheme of endogenous astrocyte $G_{i/o}$ GPCR activation by GABA. (B) Fluorescence images of an astrocyte showing selected domains in soma and processes (*top row*), pseudocolor Ca^{2+} images before and after local application of GABA (*bottom row;* scale bar, 5 μm), and Ca^{2+} traces from domains shown in top left panel (*right*). (C) *Left*: Raster plot showing Ca^{2+} events for each ROI (somas (s) below reference line, processes (p) above reference line). *Right*: Average Ca^{2+} trace from responding somas (*top*) and processes (*bottom*). T-test compares 10s before and 10s after agonist. (D and E) Ca^{2+} event probability

in somas (D) and processes (E) *vs.* time, and maximum values in different conditions. (F) Immunohistochemical images of AAV8-GFAP-hM4Di-mCherry expression in the hippocampus. *From left to right*: mCherry, GFAP, NeuN, a merge of all three, and a higher magnification merge image showing colocalization of GFAP and mCherry (25x; scale bar, 40 μm; s.o., stratum oriens; s.p., stratum pyramidale; s.r., stratum radiatum). (G-K) as (A-E) but with local application of CNO to $G_{i/o}$DREADD-expressing astrocytes instead of GABA. Data are represented as mean ± SEM. $P < 0.05$ (*), $P < 0.01$ (**), and $P < 0.001$ (***).

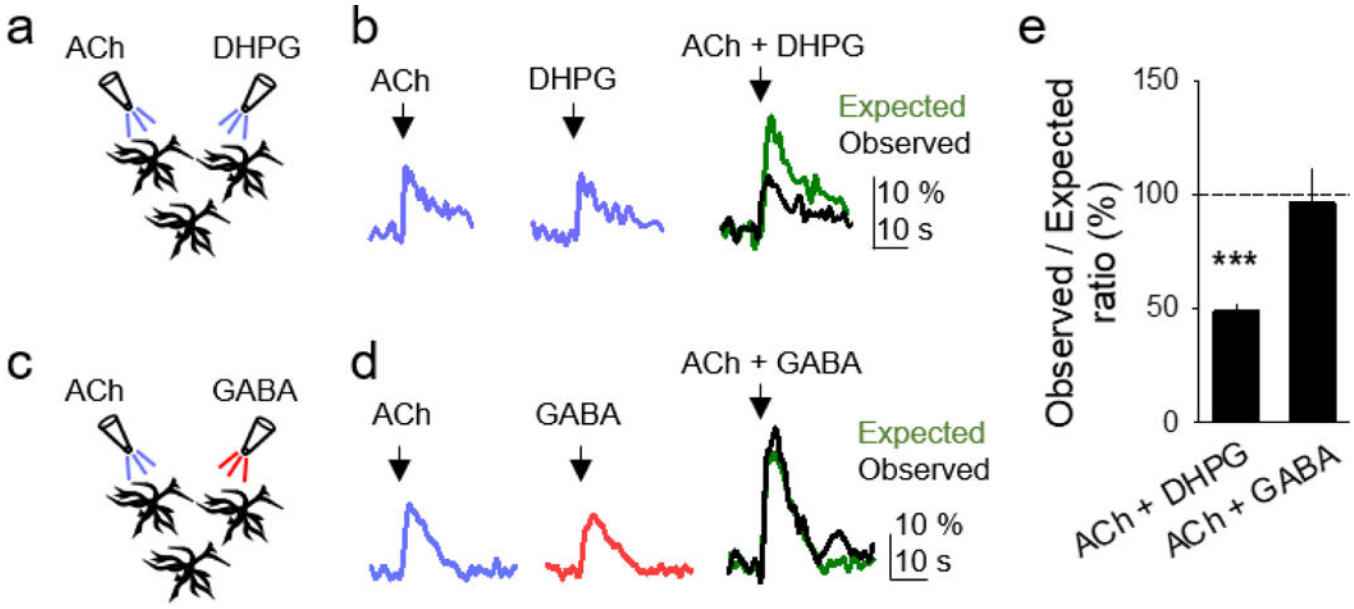

Figure 5. $G_{i/o}$ and G_q GPCRs stimulate different signaling pathways that do not occlude.
(A and B) Scheme of experimental set-up, and astrocyte Ca^{2+} responses to ACh (left), DHPG (middle), and both simultaneously (right), showing the observed (black trace) and expected (green trace) responses. Expected response corresponds to the linear summation of the responses evoked by independent application of ACh and DHPG. (C and D) as in (A and B), but with GABA instead of DHPG. (E) Histogram of the ratio of the observed and expected Ca^{2+} responses evoked by simultaneous application of GPCR agonists in the different pharmacological conditions. Expected responses were considered the linear summation of the responses elicited by independent stimulation of the agonists. Data are represented as mean ± SEM. $P < 0.001$ (***).

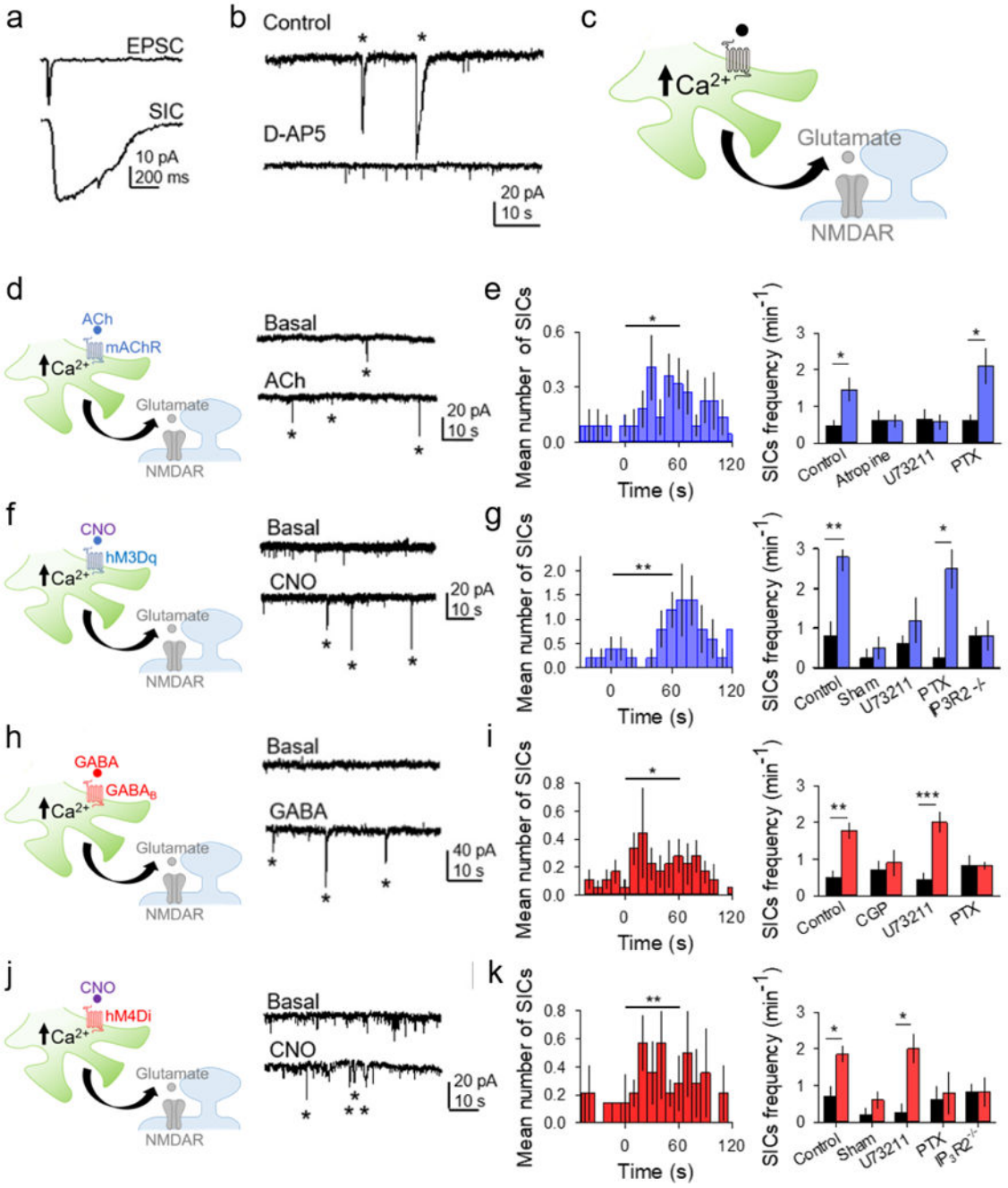

Figure 6. Astrocyte activation via G_q and $G_{i/o}$ DREADDs induces slow inward currents in neurons.

(A) Representative excitatory postsynaptic current (EPSC) and slow inward current (SIC) recorded from a CA1 pyramidal neuron. (B) Representative traces showing SICs (asterisks) in control and in D-AP5. (C) Scheme of neuronal-astroglial synaptic elements and gliotransmission. (D) Scheme and representative traces showing SICs (asterisks) before and after ACh application. (E) *Left*: Mean number of SICs *vs.* time, binned at 10s (ACh was applied at t=0). T-test compares one minute before and one minute after agonist. *Right*: SIC frequency (per min) one minute before and one minute after ACh in different conditions.

Statistical significance was determined by the Student's *t*-test comparing mean values one minute before and after agonist application. (F-G) as in (D-E) but with CNO application to G_qDREADD-expressing astrocytes. (H-I) as in (D-E) but with GABA application instead of ACh. (J-K) as in (D-E) but with CNO application to $G_{i/o}$DREADD-expressing astrocytes. Data are represented as mean ± SEM. $P < 0.05$ (*), $P < 0.01$ (**), and $P < 0.001$ (***).

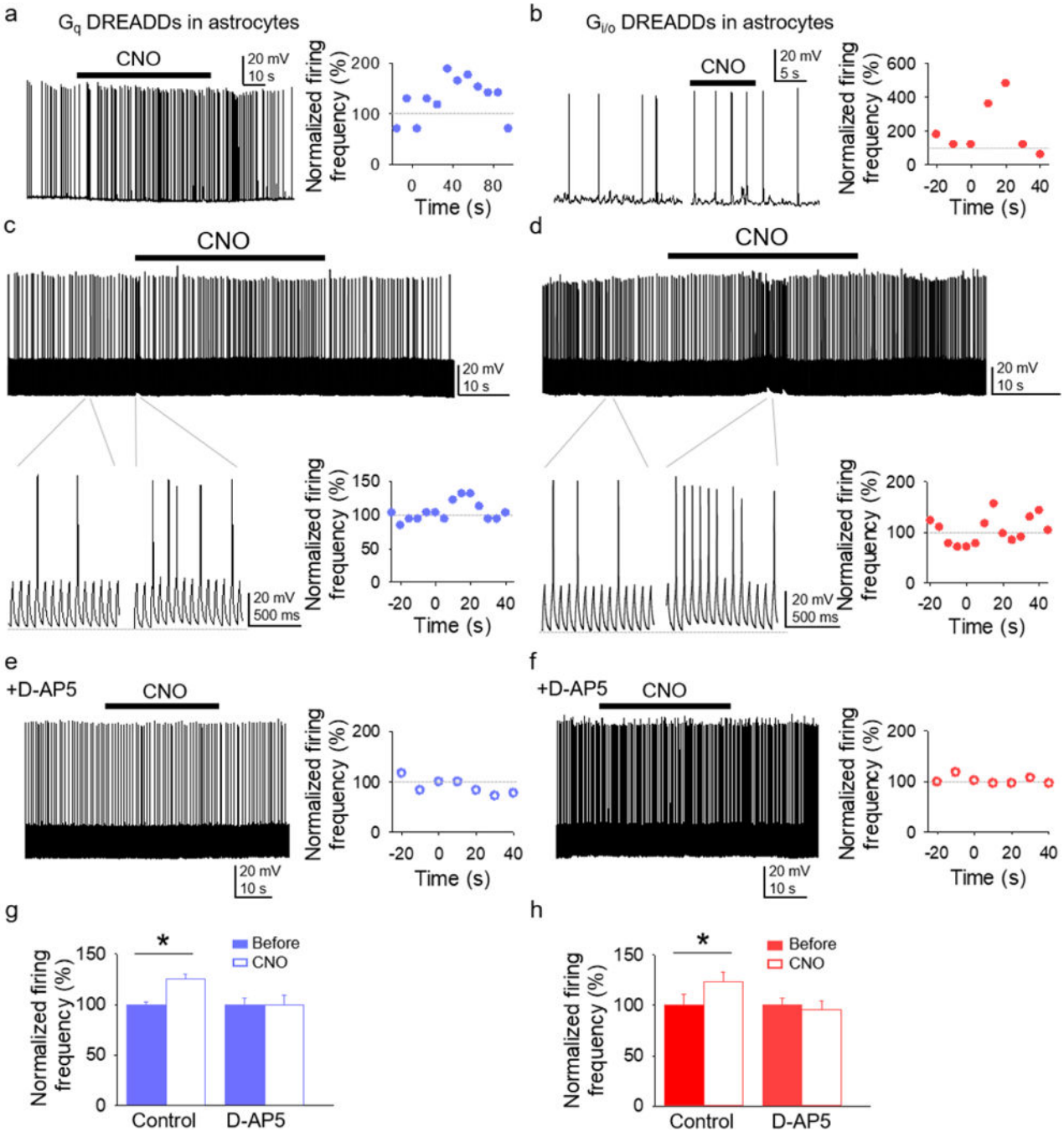

Figure 7. Astrocytic G_q and $G_{i/o}$ DREADD activation increases neuronal action potential firing.

(A and B) Representative trace of spontaneous action potential firing of CA1 pyramidal neuron before and after CNO application to G_qDREADD-expressing astrocytes (A) and $G_{i/o}$DREADD-expressing astrocytes (B), and the normalized (from basal) firing frequency *vs.* time. CNO application was at t=0 (as in the other panels). (C and D) Representative trace (*top*) of action potential firing induced by short depolarizing pulses before and after CNO application to G_qDREADD-expressing astrocytes (C) and $G_{i/o}$DREADD-expressing astrocytes (D), expanded traces (*bottom left panels*), and normalized firing frequency *vs.*

time (*bottom right panels*). (E and F) Response to CNO in the presence of D-AP5. (G and H) Normalized firing frequency before and after CNO application to G_qDREADD-expressing astrocytes (G) and G_qDREADD-expressing astrocytes (H) in control and D-AP5. Data are represented as mean ± SEM. $P < 0.05$ (*).

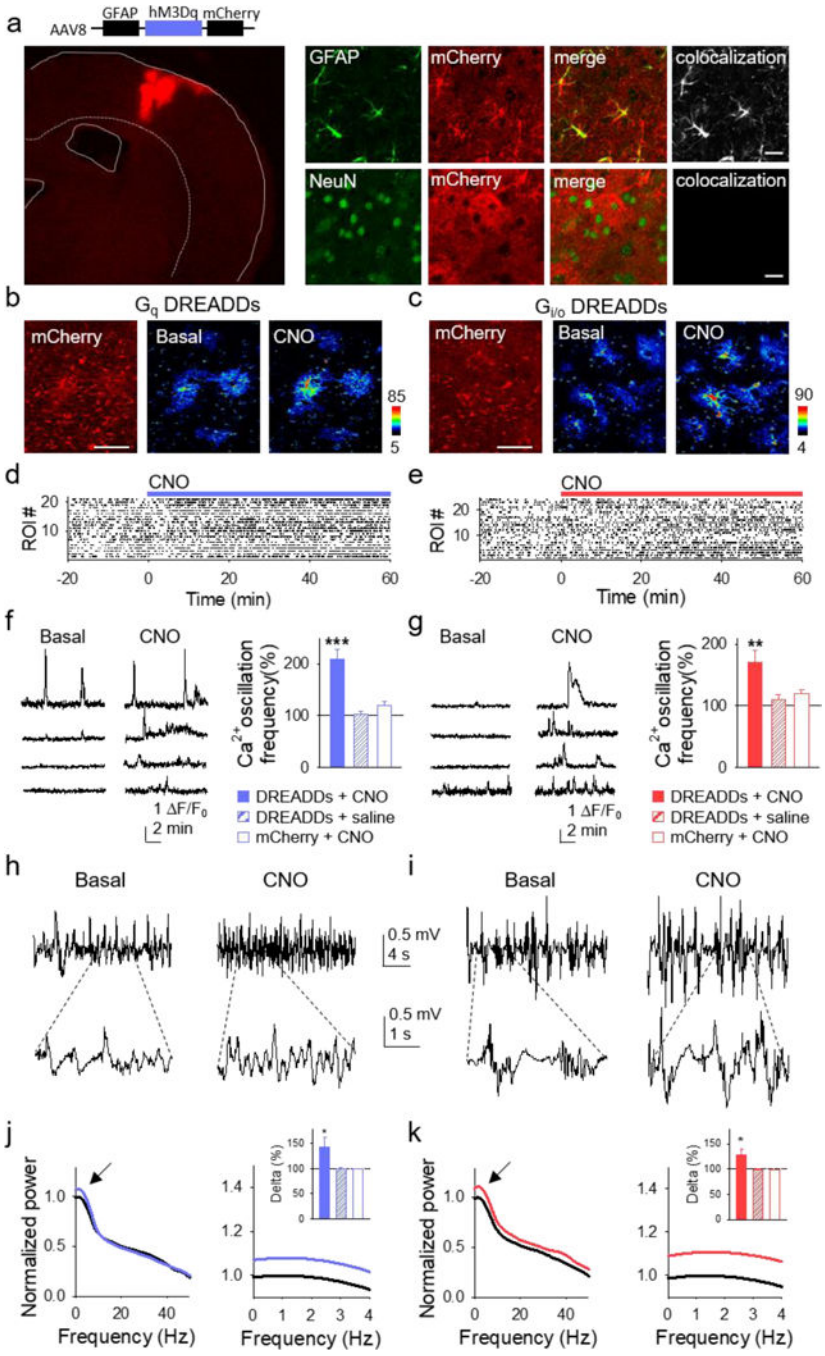

Figure 8. *In vivo* activation of both G_q and $G_{i/o}$ DREADDs in astrocytes elevates their Ca2+ levels and regulates neuronal electrical activity.

(A) Immunohistochemical representative image of G_qDREADDs virus injected into the primary somatosensory cortex staining for neurons (NeuN; *blue*), astroglia (GFAP; *green*), the reporter mCherry (*red*), and colocalization of mCherry with GFAP (top) and NeuN (bottom; scale bar, 20 μm). (B and C) *Left*: Representative images of mCherry in astrocytes reporting expression of G_qDREADDs and $G_{i/o}$DREADDs (scale bar, 50 μm). Pseudocolor Ca^{2+}images before (*middle*) and after (*right*) intraperitoneal injection (i.p.) of CNO. (D and E) Raster plots of Ca^{2+} events before and after i.p. injection of CNO in mice with astrocytes

expressing G_q and $G_{i/o}$DREADDs, respectively. (F and G) Representative Ca^{2+} traces during basal (*left*) and after i.p. CNO injection (*right*) in G_qDREADD- (F) and $G_{i/o}$DREADD-injected (G) mice. Ca^{2+} oscillation frequency normalized to baseline for DREADDs-infected cortex with i.p. CNO injections (solid bars), for DREADDs-infected cortex with i.p. saline injections (hashed bars), and for mCherry control-infected cortex with i.p. CNO injections (unfilled bars) for G_qDREADDs- (F) and $G_{i/o}$DREADDs-injected (G) mice. (H and I) Representative cortical local field potential recordings prior to CNO (*left*) and after (*right*) in G_qDREADDs- (H) and $G_{i/o}$DREADDs-injected (I) mice. Lowpass filtered at 40Hz. (J and K) Normalized power spectrum of cortical local field potentials before (black) and after CNO in G_qDREADDs- (J: blue) and $G_{i/o}$DREADDs-injected (K: red) mice. Normalized power spectrum of slow-wave delta (0–4 Hz) activity for DREADDs-infected cortex with i.p. CNO injections (solid bars), DREADDs-infected cortex with i.p. saline injections (hashed bars), and mCherry control-infected cortex with i.p. CNO injections for G_qDREADDs- (J) and $G_{i/o}$DREADDs-injected (K) mice. Error bars are SEM. $P < 0.05$ (*), $P < 0.01$ (**), and $P < 0.001$ (***).